

RESEARCH ARTICLE

Species-specific function of conserved regulators in orchestrating rice root architecture

Tushar Garg^{1,*}, Zeenu Singh^{1,*}, Kunchapu Chennakesavulu^{1,‡}, Khrang Khrang Khungur Mushahary^{1,‡}, Anuj Kumar Dwivedi^{2,‡}, Vijina Varapparambathu^{3,4,‡}, Harshita Singh¹, Raj Suryan Singh¹, Debabrata Sircar¹, Divya Chandran⁵, Kalika Prasad^{3,4}, Mukesh Jain² and Shri Ram Yadav^{1,§}

ABSTRACT

Shoot-borne adventitious/crown roots form a highly derived fibrous root system in grasses. The molecular mechanisms controlling their development remain largely unknown. Here, we provide a genome-wide landscape of transcriptional signatures – tightly regulated auxin response and in-depth spatio-temporal expression patterns of potential epigenetic modifiers – and transcription factors during priming and outgrowth of rice (*Oryza sativa*) crown root primordia. Functional analyses of rice transcription factors from WUSCHEL-RELATED HOMEBOX and PLETHORA gene families reveal their non-redundant and species-specific roles in determining the root architecture. *WOX10* and *PLT1* regulate both shoot-borne crown roots and root-borne lateral roots, but *PLT2* specifically controls lateral root development. *PLT1* activates local auxin biosynthesis genes to promote crown root development. Interestingly, *O. sativa* PLT genes rescue lateral root primordia outgrowth defects of *Arabidopsis plt* mutants, demonstrating their conserved role in root primordia outgrowth irrespective of their developmental origin. Together, our findings unveil a molecular framework of tissue transdifferentiation during root primordia establishment, leading to the culmination of robust fibrous root architecture. This also suggests that conserved factors have evolved their transcription regulation to acquire species-specific function.

KEY WORDS: Adventitious/crown root primordia, RNA *in situ* hybridization, Laser capture microdissection, Lateral root, *Oryza sativa*, Transcription factors

INTRODUCTION

Unlike the taproot system in dicot plants, monocot grass species (*Poaceae* or *Gramineae* family) develop a highly diversified fibrous root system. The cereal crops such as rice (*Oryza sativa*), maize (*Zea mays*), wheat (*Triticum aestivum*) and barley (*Hordeum vulgare*) from this family are major food sources worldwide. They develop

various types of post-embryonic adventitious roots (ARs) from non-root tissues under normal and stress conditions (Atkinson et al., 2014; Steffens and Rasmussen, 2016). The rice root system is mainly composed of shoot-borne crown roots (CRs), whereas in maize, both subterranean CRs and aerial brace roots (BRs) are shoot-borne ARs (Itoh et al., 2005; Meng et al., 2019; Bellini et al., 2014; Hostetler et al., 2021). Lateral roots (LRs) are root-borne post-embryonic roots that develop from the primary roots (PRs), seminal roots and ARs. The origin of various post-embryonic roots is highly variable in plant species. For example, ARs arise from the pericycle cells at the xylem pole of *Arabidopsis* hypocotyl but from differentiated phloem cells in tomato (Bellini et al., 2014; Omary et al., 2022). However, in monocot grass species, such as rice and maize, CRs are developed from the innermost ground tissues peripheral to the vascular cylinder at the stem base (Itoh et al., 2005; Bellini et al., 2014). Similarly, LRs originate from the xylem pole pericycle cells of the *Arabidopsis* PR, whereas the endodermal and pericycle cells located opposite to the protophloem of the PR and CRs produce LRs in grasses (Itoh et al., 2005; Orman-Ligeza et al., 2013; Atkinson et al., 2014; Bellini et al., 2014).

Auxin signaling and its cross-talk with transcription factors (TFs) and other signaling pathways have been instrumental for founder cell specification and root organogenesis in plants (Lavenus et al., 2013; Hochholdinger et al., 2018; Li et al., 2019; Meng et al., 2019; Neogy et al., 2019; Li, 2021). Despite gross morphological and anatomical similarities among various root types, certain genetic regulators display specific and unequal roles in different types of roots (Hochholdinger et al., 2004, 2018; Coudert et al., 2010; Kitomi et al., 2011a,b; Orman-Ligeza et al., 2013; Atkinson et al., 2014; Li et al., 2019; Meng et al., 2019). For example, *Arabidopsis* LOB-domain containing TF LBD29 is primarily involved in regulating root-borne LR initiation (Okushima et al., 2007), whereas its rice homolog ADVENTITIOUS ROOTLESS 1 [ARL1; also known as CROWN ROOTLESS 1 (CRL1)] mainly regulates shoot-borne CR initiation with lesser effects on LR development (Inukai et al., 2005; Liu et al., 2005). Maize CRL1 homolog RTCS controls seminal and shoot-borne roots (i.e. CRs and BRs) but has no significant role in LR formation (Hetz et al., 1996). The function of CRL1 homologs in the regulation of shoot-borne root initiation is also conserved in tomato and potato (Omary et al., 2022). A maize AP2-domain TF, RAP2.7, specifically controls aerial shoot-borne BR development without affecting subterranean shoot-borne CR formation (Li et al., 2019). However, it remains unexplored how such conserved factors acquire a species-specific and unequal role in different root types to bring morphological diversity in the root architecture.

The establishment of rice shoot-borne crown root primordia (CRP) requires an induction phase for cell cycle reactivation in a localized domain of the stem innermost ground tissues to produce

¹Department of Biosciences and Bioengineering, Indian Institute of Technology Roorkee, Uttarakhand 247667, India. ²School of Computational and Integrative Sciences, Jawaharlal Nehru University, New Delhi 110067, India. ³School of Biology, Indian Institute of Science Education and Research, Thiruvananthapuram 695001, Kerala, India. ⁴School of Biology, Indian Institute of Science Education and Research, Pune 411007, Maharashtra, India. ⁵Laboratory of Plant-Microbe Interactions, Regional Center for Biotechnology, Faridabad, Haryana 110076, India.

*These authors contributed equally to this work

‡These authors contributed equally to this work

§Author for correspondence (shri.yadav@bt.iitr.ac.in)

DOI: M.J., 0000-0002-7622-1083; S.R.Y., 0000-0002-4083-7054

CRP founder cells (Itoh et al., 2005; Guan et al., 2015). Later, these CRP founder cells divide and their daughter cells differentiate into root tissues (Itoh et al., 2005). However, the global gene architecture and gene regulatory modules during CRP initiation and differentiation have not yet been fully uncovered. Here, we characterize a variety of genetic and epigenetic regulators identified through laser capture microdissection-RNA-sequencing (LCM-seq) of developing shoot-borne CRP. We show that spatio-temporal reorganization of these regulators is key to progressive development of shoot-borne root primordia in rice. The functional studies demonstrate that a few members of the WUSCHEL-RELATED HOMEBOX (WOX) and PLETHORA (PLT) gene families control rice root architecture. *PLT1* has acquired species-specific function in controlling shoot-borne root (CR) development while retaining its conserved function of regulating root-borne root (LR) outgrowth. Interestingly, *PLT2* is exclusively deployed in controlling lateral root development, suggesting functional specificity amongst the related members of a gene family. Our findings provide insights into how related members of a large gene family have evolved towards functional innovation in addition to their conserved role in grasses.

RESULTS

Laser microdissection and global gene expression profile of developing rice CRP

Rice CRP establishment begins with an initiation stage, in which founder cells for the primordia are specified by virtue of shoot-to-root cell fate conversion followed by the specification of initial cells for epidermis-endodermis, root cap and central stele (Fig. 1A,B; Itoh et al., 2005). Subsequently, the stem cell niche organization leads the CRP progression to the outgrowth stage, during which tissue organization and patterning advance CR formation (Fig. 1A,B). Generation of the essential auxin maxima is a prerequisite for root primordia formation (Benková et al., 2003; Dubrovsky et al., 2008; De Rybel et al., 2010; Omary et al., 2022). Thus, we studied the spatio-temporal activation of auxin signaling by monitoring auxin response during rice CRP development. Our RNA *in situ* hybridization using antisense YFP RNA probes (Fig. 1Ca-Cc) and immunohistochemistry analyses with anti-GFP antibodies (Fig. 1Cd,Ce) reported a strong auxin response during CRP initiation in the rice lines expressing the DR5-erYFP construct, whereas no signal was detected in the CRP of wild-type plants (Fig. 1C; Fig. S1). However, in outgrowing CRP, auxin signaling is largely confined at the tip of the primordia (Fig. 1C), and eventually restricted to quiescent center (QC), columella and initial cells of the emerged root tip (Yang et al., 2017). Our data suggest that the auxin response is activated at the onset of CRP initiation and eventually culminates in robust auxin signaling in the spatially restricted domains during primordia outgrowth.

To dissect the determinants of cell fate change and primordia differentiation, we performed LCM-seq of developing CRP and generated a high-resolution temporal gene expression map of rice shoot-borne CRP at their progressive developmental stages; CRP initiation and CRP outgrowth (Fig. 1D). Before organization of the fundamental tissues, eleven CRP with overlapping stages of primordia specification and division of tissue initial cells were microdissected from cross-sections of the rice stem base and pooled for the CRP initiation stage (Fig. 1B, left and middle panels). For the CRP outgrowth stage, we collected ten CRP in which stem cell niche, fundamental and vascular tissues were patterned (Fig. 1B, right panel). The ground tissues peripheral to the vascular cylinder at the stem base, competent to develop CRP, were collected as control (Fig. 1D). RNAs extracted from the CRP were subjected to

RNA-seq. The analysis of various quality control parameters (Fig. S2A-F) and the expression pattern of known marker genes expressed during rice CR development (Table S1) confirmed the good quality of the RNA-seq data.

Patterns of gene expression and associated biological processes during CRP development

The global gene expression profiling and fuzzy c-means clustering of LCM-seq transcriptomic data yielded eight clear clusters with distinct gene expression patterns (Fig. 2A; Table S2). Each cluster pattern was associated with specific biological processes correlated to gene expression, DNA replication, cell cycle regulation, hormonal signaling and development, showing the apparent molecular and cellular remodeling required for cell fate switching and root tissue differentiation in CRP (Fig. 2B). The differential gene expression analysis identified genes exclusively or commonly expressed (\log_2 fold change ≥ 1 or ≤ -1 , q -value < 0.05) during CRP initiation and outgrowth, thus providing CRP stage-specific molecular signatures (Fig. 2C; Tables S3,S4). Upon overlapping differentially expressed genes (DEGs) in the CoNekT database, we noted that the larger fraction of CRP-activated genes showed a higher expression (z -score > 0) in the actively dividing meristematic zone (Fig. 2D), whereas the repressed genes were largely expressed in the differentiation zone of emerged CRs (Fig. 2E).

Further, gene ontology (GO) enrichment analysis of the obtained DEGs provided a deeper insight into the key biological processes associated with CRP development (Fig. S3). Notably, the CRP initiation stage was solely enriched with genes regulating hormonal levels, transcription pre-initiation, RNA processing, cell cycle and organ development, whereas primary metabolic processes were linked with the genes particularly induced during CRP outgrowth (Fig. S3A). Similarly, biological processes related to hormonal signaling, gene regulation, cell division and post-embryonic root organogenesis were associated with genes with higher expression in the initiating CRP compared with the outgrowing CRP (Fig. S3B). Collectively, this suggests that the key biological processes required for CRP establishment and differentiation are co-related with genes highly expressed during CRP initiation.

Transcriptional activation of epigenetic modifiers during CRP development

The geneset enrichment analysis (GSEA) of transcriptome data identified CRP stage-specific molecular signatures of epigenetic modifiers (Fig. S4A). Noticeably, PHD, SWI/SNF, SET, GNAT and Jumonji gene families (putative epigenetic and chromatin remodeling factors) were largely induced during CRP initiation (Fig. S4A; Table S5), suggesting a crucial requirement of chromatin remodeling for transcriptional reprogramming for cell fate transition and new organ initiation. Therefore, to validate induced expression of these factors and to uncover their onset of activation during CRP establishment, we examined the spatial and temporal expression pattern of three candidate epigenetic modifiers; two PHD-domain containing chromatin-remodeling factors [TRX1 (Os09g04890) and ATXR6 (Os01g73460)], and a SWIB complex BAF60b domain-containing protein, [SWIB/BAF60b (Os03g55310)]. PHD-domain-containing proteins are epigenetic effectors that recognize trimethylated histone H3 and recruit histone acetyl transferase (HAT) or histone deacetylase (HDAC) complexes, regulating transcriptional activation or repression of genes during plant development (López-González et al., 2014; Mouriz et al., 2015). However, the *Arabidopsis* BAF60 subunit of SWI/SNF chromatin-remodeling complex directly changes chromatin

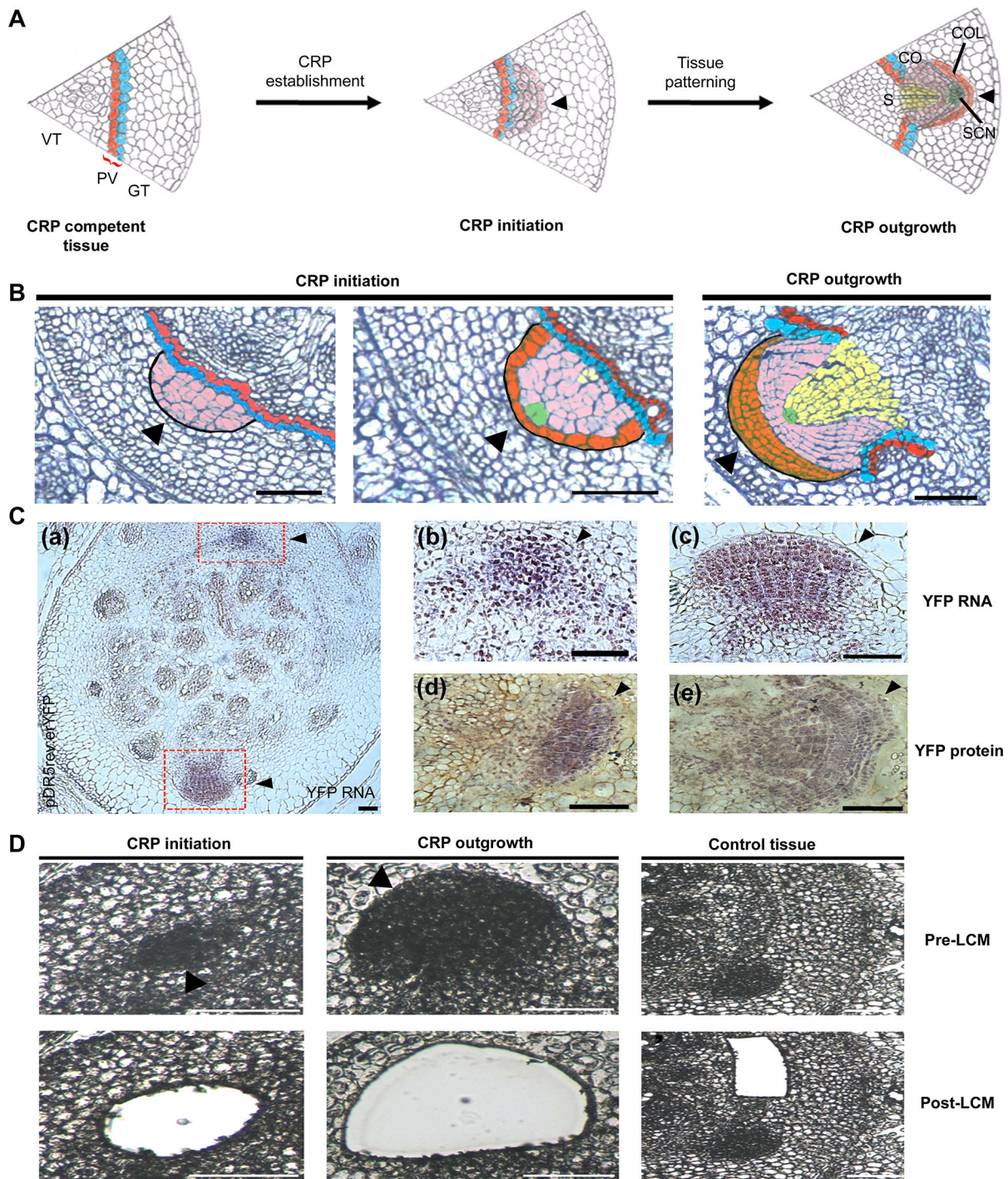


Fig. 1. Auxin response and laser capture microdissection in developing shoot-borne rice crown root primordia. (A) Schematic showing crown root primordia (CRP)-competent tissues and developing CRP at the stages of initiation and outgrowth. CO, cortex; COL, columella; GT, ground tissues; PV, peripheral tissues of vascular cylinder; S, stele; SCN, stem cell niche; VT, vascular tissues. (B) Cross-sections of 6-day-old rice stem base showing the stages of CRP initiation (left and middle panels) and subsequent outgrowth (right panel). Stem cell niche (green), root cap tissues (orange), ground tissues (pink), endodermis (blue), pericycle (red), and vascular tissues (yellow) are highlighted in the CRP. (C) Auxin response pattern during rice CRP development using pDR5rev::eYFP construct. RNA *in situ* hybridization with antisense YFP riboprobes (Ca-Cc) and immunohistochemistry with anti-GFP antibody (Cd,Ce) are shown. CRP marked in the red box in Ca are enlarged in Cb and Cc. (D) Rice CRP (pre- and post-laser capture microdissection) during their initiation (left panels) and outgrowth (middle panels) stages. Innermost ground tissues competent for CRP initiation were collected as control tissues (right panels). Black arrowheads mark CRP. Scale bars: 50 μ m.

conformation of the *FLOWERING LOCUS C* (*FLC*) gene (Jégu et al., 2014). In LCM-seq data, the expression of these selected genes was sharply induced during CRP initiation but declined at the later stage of CRP outgrowth (Fig. S4B-D). Our RNA *in situ* hybridization validated their expression patterns in the developing

CRP and also uncovered an early transcriptional onset of these epigenetic modifiers in the CRP founder cells and their descendants (Fig. 3A; Table S6).

Further, to provide functional support towards the involvement of epigenetic regulation in controlling the grass root system, we

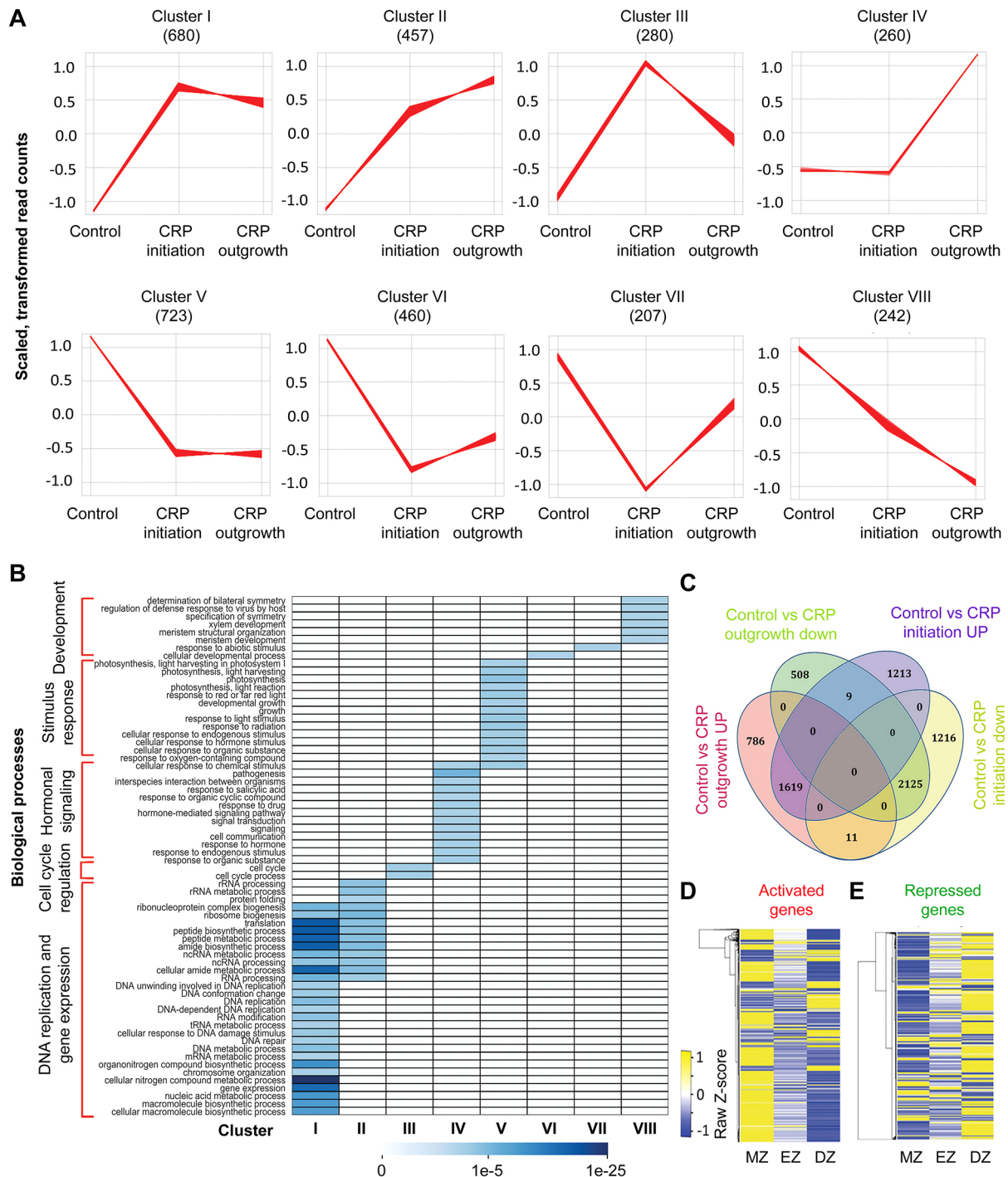


Fig. 2. RNA-seq data analysis of laser capture microdissection-captured rice CRP. (A) Gene expression patterns (scaled, transformed read counts on y-axis) of laser capture microdissection-acquired CRPs at initiation and outgrowth (x-axis) stages show eight definite clusters (I–VIII). (B) Heatmap of distinct GO terms enrichment associated with different biological processes in eight gene clusters (I–VIII). The log₂ fold enrichment ≥ 1 with $P < 0.05$ was considered and P -value (scale bar: 0 to $1e-25$) was used to generate the heatmap. (C) Venn diagram of common and unique differentially expressed genes (DEGs) during CRP initiation and outgrowth. (D, E) Hierarchical clustering heatmap of activated (D) and repressed (E) DEGs using raw z-score values (scale bar: -1 to 1) in different zones of emerged roots, analyzed from the CoNekT database. MZ, meristematic zone; EZ, elongation zone; DZ, differentiation zone.

interfered with the processes of epigenetic modification. We observed an altered root architecture upon chemical interference of histone acetylation and DNA methylation. Induced histone acetylation either by promoting histone acetylation (by exposing with sodium acetate) or inhibiting histone deacetylase activities (by treating with sodium butyrate) resulted in a reduced CR number (Fig. 3B,C; Fig. S4E,F). In contrast, inhibition of DNA methylation

using 5-azacitidine displayed an increased CR number (Fig. 3B,C). Next, to test whether the expression of CRP-expressed TFs identified from our LCM-seq data was affected upon epigenetic interference, we analyzed expression of ten selected key TFs upon chemical treatments. We observed that the expression of many of these TFs was altered upon sodium acetate and/or 5-azacitidine treatments (Fig. 3D). In accordance with the opposite effects of

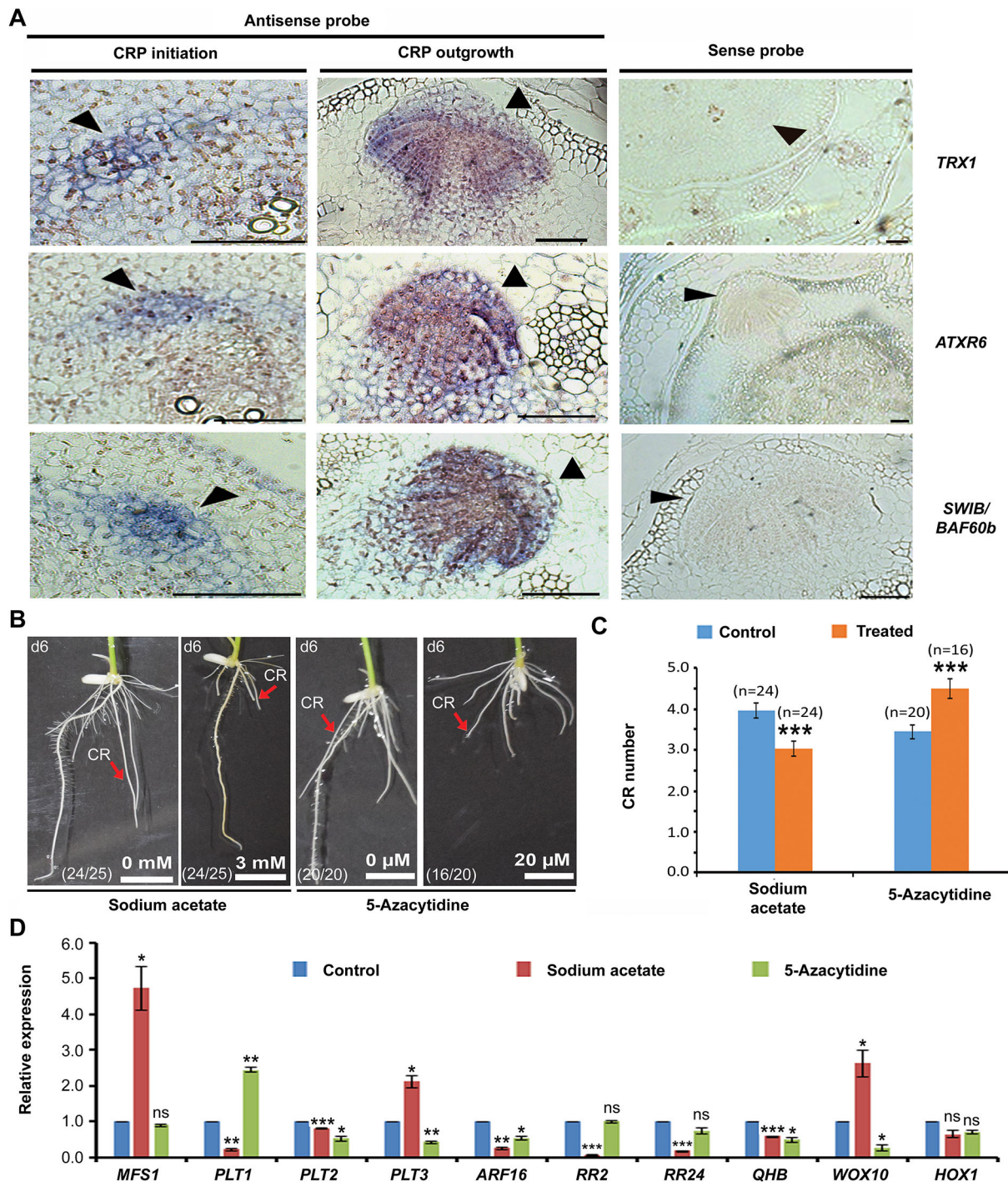


Fig. 3. Epigenetic regulation of rice root architecture. (A) Tempo-spatial expression pattern of three putative epigenetic regulators, *TRX1*, *ATXR6* and *SWIB/BAF60b*, in developing crown root primordia (CRP). All these genes are activated at the onset of CRP initiation (left panels), with continued expression in outgrowing CRP (middle panels). Cross-sections of 6-day-old rice stem base were hybridized with anti-sense (left and middle panels) and sense (right panels) RNA probes. (B) Interference in histone acetylation (by treating with sodium acetate) or DNA methylation (by treating with 5-azacytidine treatment) resulted an altered root architecture. CR, crown roots. (C) Quantitative representation of CR number upon treatments with these drugs. CR number is inversely affected in the 6-day-old seedlings upon induction of histone acetylation ($n=24$) and inhibition of DNA methylation ($n=16$). Data are mean CR number \pm s.e.m. ($***P \leq 0.001$; two-tailed unpaired Student's *t*-test). Sample size (n) is shown in panels. (D) Expression level of ten selected CRP-expressed transcription factors in rice stem base upon pharmacological interference of histone acetylation and DNA methylation for 6 days. Relative expression (fold change) is plotted \pm s.e.m. The *P*-value is calculated from three experiments (ns, not significant, $P > 0.05$; $*P \leq 0.05$; $**P \leq 0.005$; $***P \leq 0.001$; two-tailed unpaired Student's *t*-test). The expression of *WOX10*, *PLT1* and *PLT3* is altered in an opposite manner upon treatment with sodium acetate and 5-azacytidine. The site of CRP establishment and developing CRP are highlighted with black arrowheads in A. Red arrows mark the CR in B. Scale bars: 50 μ m (A); 1 cm (B).

sodium acetate and 5-azacytidine treatments on CR number, the expression of *PLT1*, *PLT3* and *WOX10* was changed in an inverse manner (Fig. 3D). These data together indicate that early activation

of epigenetic regulators during CRP establishment can modulate expression dynamics of a set of cell fate determinants during CRP initiation.

Spatio-temporal expression dynamics of transcription factors in developing CRP

TFs are master regulators of cell fate determination during organogenesis. We identified TFs specifically and commonly expressed (\log_2 fold change ≥ 1 or ≤ -1 , q -value < 0.05) in the initiating and outgrowing CRP (Fig. S5A; Table S7). The TFs sharply and transiently induced during CRP initiation might be required for initiating CRP-specific genetic programs. However, TFs which were specifically induced or maintained in outgrowing CRP might control meristem maintenance and tissue patterning.

To further validate LCM-seq expression pattern and reveal expression dynamics of key TFs in developing CRP, we examined spatial and temporal expression patterns of seven representative TFs from various gene families known to be involved in regulating organ initiation and development. This list included three TFs from the AP2-ERF gene family (*ERF3*, *PLT1* and *PLT2*), an auxin response factor (*ARF16*), a cytokinin response regulator (*RR24*) and two homeobox TFs (*WOX10* and *HOX1*). The expression of *ERF3* (*Os01g58420*), *ARF16* (*Os06g09660*), *RR24* (*Os02g08500*), *WOX10* (*Os08g14400*) and *HOX1* (*Os10g41230*) was sharply induced during CRP initiation but was eventually reduced in the outgrowing CRP in LCM-seq data (Fig. S5B-F; Table S6). However, the expression of *PLT1* (*Os04g55970*) and *PLT2* (*Os06g44750*) was induced in initiating CRP and maintained during CRP outgrowth (Fig. S5G,H; Table S6). Our RNA *in situ* hybridization confirmed specific and strong expression of all chosen TFs in the developing CRP (Fig. 4, left and middle panels), whereas the tissues hybridized with sense probe did not show any expression signal above background level (Fig. 4, right panels). The expression of these factors commenced in a localized domain of ground tissues peripheral to the vascular tissues during CRP initiation (Fig. 4, left panels) and they were consistently expressed in the outgrowing primordia (Fig. 4, middle panels). These results confirm that the expression of a set of key transcriptional regulators is confined to developing CRP and suggest a strict necessity of their spatial regulation during CR development.

WOX10 controls timely initiation and growth of rice roots

Arabidopsis *WOX11* and *WOX12*, members of the WOX gene family, regulate cell fate transition during *de novo* root organogenesis (Liu et al., 2014). Of the three rice members of the *WOX11/12* sub-clade (Fig. 5A), we found that the expression of *WOX10* was sharply and transiently activated during CRP initiation (Fig. S5E; Table S6). Its expression was also altered upon sodium acetate and 5-azacitidine treatments in an opposite manner (Fig. 3D). Our spatio-temporal expression analysis of *WOX10* demonstrated that its transcription was activated in the founder cells of CRP, before their establishment (Fig. S6A). All these observations together pointed to *WOX10* as a potential regulator of CRP initiation; we therefore chose it for detailed functional characterization.

To investigate the function of *WOX10* during rice CR development, we generated both loss- and gain-of-function rice transgenic lines. An inverted repeat RNA-interference (RNAi) construct was expressed in rice using the estradiol-inducible XVE system (*pUbi::XVE:dsWOX10*) to downregulate endogenous expression of *WOX10*. Estradiol (17- β)-induced knockdown of *WOX10* resulted in delayed CR formation in rice plants (Fig. 5B,C; Fig. S6B,C). Both CR number and length were reduced in downregulated lines during early stages (Fig. 5B,C; Fig. S6B,C). At later stages, the number of CRs was not significantly altered (Fig. S6F), but the length of CRs and LR was reduced upon *WOX10* downregulation, thus altering overall root architecture

(Fig. 5D-F; Fig. S6D,E). The expression of *WOX10* was reduced in downregulated plants but no significant change was observed in the expression of the related WOX genes *WOX11* and *WOX12* (Fig. S6G), confirming specificity of downregulation. In contrast, ectopic expression of *WOX10* under the maize ubiquitin promoter (*pUbi::WOX10*) in rice lines caused the opposite effect of increased CR number (Fig. 5G,H; Fig. S7A-D). Occasionally, precocious CR formation was observed in *pUbi::WOX10* plants (Fig. S7E). The length of CRs and LR was also inversely affected in ectopic expression lines (Fig. 5G; Fig. S7A-C). A strong overexpression of *WOX10* was confirmed by RT-PCR analyses (Fig. S7F,G). These observations suggest that *WOX10* promotes initiation as well as subsequent growth of post-embryonic roots in rice plants.

PLT1 controls shoot-borne CR and root-borne LR development in rice

AP2-domain containing PLT genes are among key cell fate determinants of root growth and development (Aida et al., 2004; Galinha et al., 2007). In the LCM-seq data, we noticed a sharp transcriptional activation of six rice PLT genes (*PLT1-PLT6*) in shoot-borne CRP (Fig. S8A; Table S6). In *Arabidopsis*, three PLT genes redundantly regulate root-borne LR outgrowth (Du and Scheres, 2017). Rice root architecture considerably differs from *Arabidopsis* in having both shoot-derived CRs and root-derived LR (Bellini et al., 2014). However, it remains unknown whether any of these PLT genes has acquired species-specific function in regulating adventitious roots in plants (Li and Xue, 2011). Investigation of spatio-temporal expression pattern of *PLT1* in rice CR elucidated that its transcription was activated at the onset of CRP specification (Fig. S8B). The expression of *PLT1* was also altered upon pharmacological interference of epigenetic processes (Fig. 3D).

To chart the function of *PLT1* in rice root development, we created its both loss- and gain-of-function transgenic rice lines. In *PLT1* downregulated rice lines (*dsRNAiPLT1*), the root architecture was notably compromised (Fig. 6A,B), as indicated by the shortened length of all root types (i.e. pole-borne PR, shoot-borne CR and root-borne LR) (Fig. 6A; Fig. S8C-E). In addition, the number of CRs and CRPs, and LR was also substantially decreased in these knockdown lines (Fig. 6B-D; Fig. S8C-E) because of dismissed CRP initiation at the stem base. The extent and specificity of *PLT1* downregulation was confirmed by qRT-PCR with no significant effect on other related rice PLT genes (Fig. S8F). This concludes that, unlike *Arabidopsis* PLTs, *PLT1* is indispensable for shaping root architecture in rice. Further, in a complementary approach, we used inducible transgenic rice line *PLT1-GR*, overexpressing *PLT1* in fusion with the c-terminal domain of the glucocorticoid receptor (GR). As opposed to the phenotypes of *dsRNAiPLT1* knockdown lines, growing *PLT1-GR* (lines L#1, L#3 and L#6) plants in the presence of dexamethasone (dex) resulted in a more robust root system compared with mock-treated plants (Fig. 6E; Fig. S9A; Fig. S11B). The number of shoot-borne CRs was significantly increased in multiple independent *PLT1-GR* overexpression rice lines (both in T1 and T2 generations) in the presence of dex, with no comparable change in wild-type CR numbers (Fig. 6F; Fig. S9B). Moreover, CRs, particularly younger roots and PRs (marked with red arrowheads), developed a higher density of longer LR post-dex induction, in correlation with mock-treated plants (Fig. 6E; Fig. S9A,C). Notably, the origin of CRs (shoot borne; innermost ground tissues at stem base) and LR (root-borne; endodermal-pericycle cells located opposite to protophloem of PR and CR) have diverged in rice. The expression of *PLT1-GR*

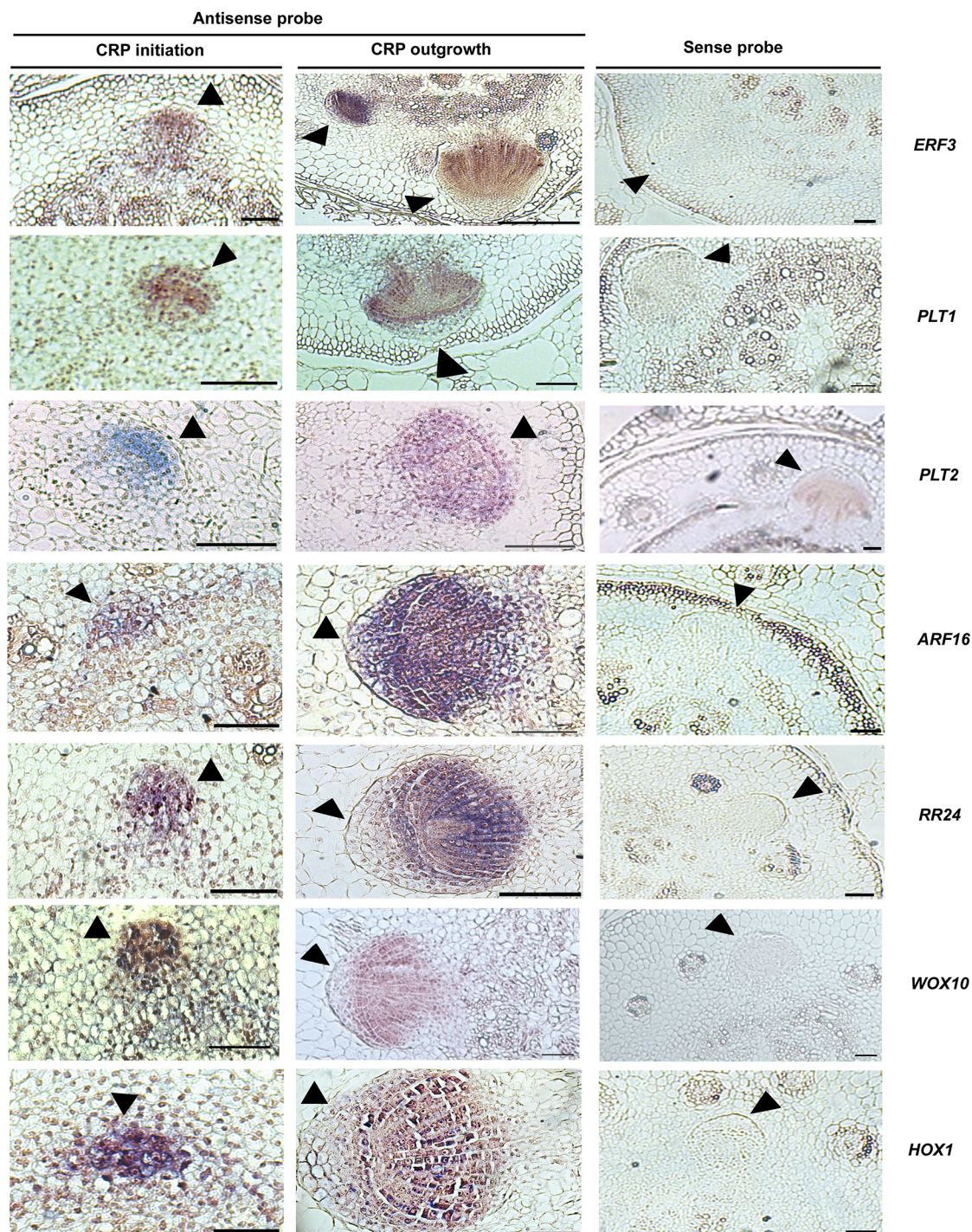


Fig. 4. Tempo-spatial expression pattern of selected transcription factors during crown root primordia development in rice. RNA *in situ* hybridization of seven selected key transcription factors (TFs), *ERF3*, *PLT1*, *PLT2*, *ARF16*, *RR24*, *WOX10* and *HOX1*, during initiation- (left panels) and outgrowth- (middle panels) stage crown root primordia (CRP). Developing CRP in the stem base of 6-day-old rice plants, probed with DIG-labeled antisense RNA probes (left and middle panels) of respective genes displayed dynamic and CRP-specific strong expression. In contrast, CRP probed with DIG-labeled sense riboprobes did not show the expression above the background, confirming specific expression of the genes. Initiating and developing CRP are highlighted with black arrowheads. Scale bars: 50 μ m.

fusion transcript was confirmed in *PLT1-GR* lines by RT-PCR analysis (Fig. S11D). These outcomes reveal that *PLT1* non-redundantly promotes post-embryonic root development in rice, irrespective of the tissue origin. Further, the results suggest that *PLT1* has an additional function of promoting CR development in rice, while retaining its conserved role in LR development.

***PLT2* specifically promotes root-borne LR development in rice**

Next, to study functional divergence among rice *PLT* genes, we functionally characterized another member, *PLT2*. As *PLT2* is the closest homolog of *Arabidopsis* *PLT5* (Luong et al., 2021), which functions redundantly with *PLT3* and *PLT7* (Prasad et al., 2011;

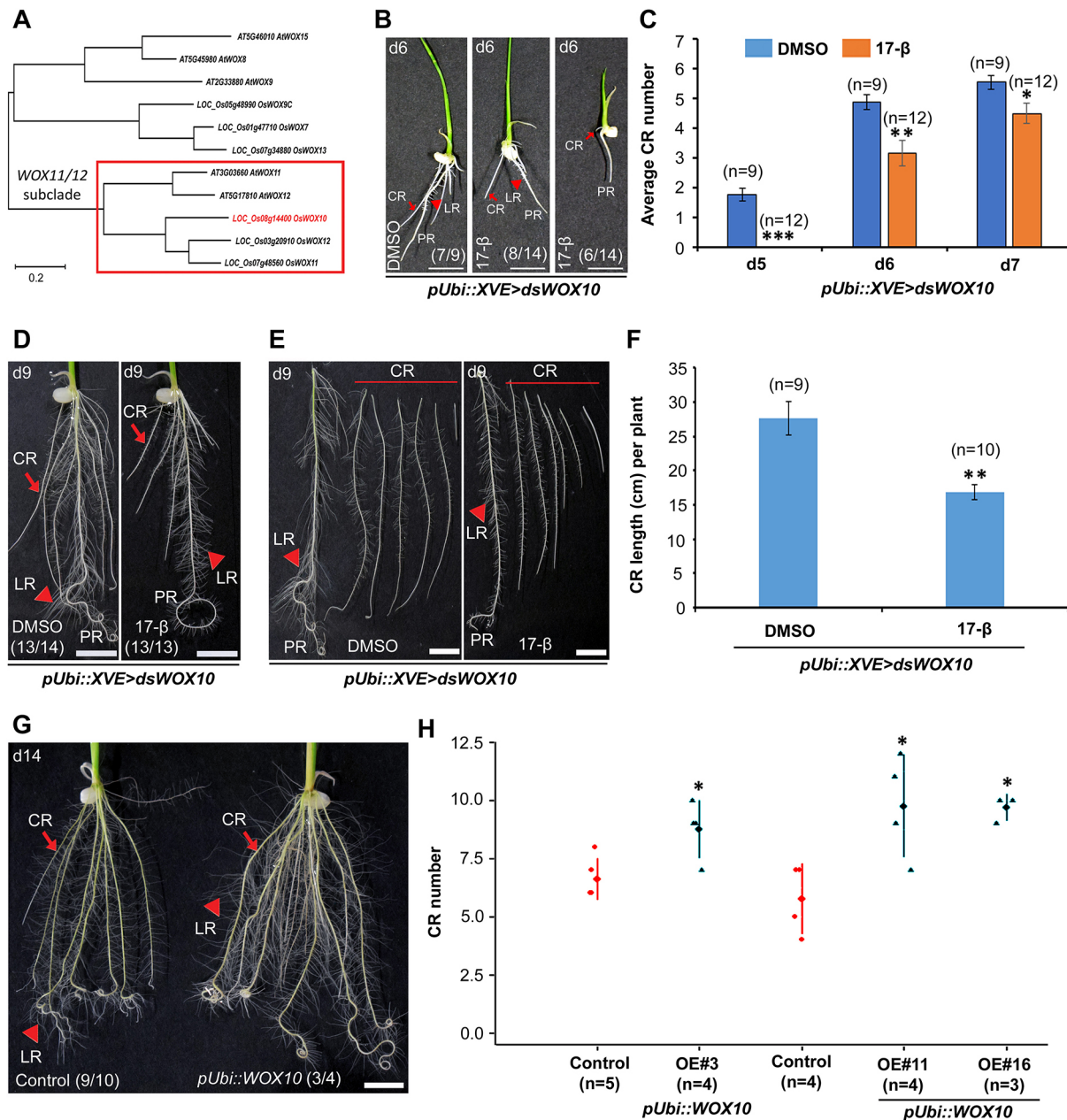


Fig. 5. *WOX10* promotes rice post-embryonic root development. (A) Phylogenetic analysis of WOX members of the intermediate clade showed that *WOX10* (red) is closely related to *Arabidopsis* *WOX11* and *WOX12*. (B) Altered root architecture in 6-day-old *pUbi::XVE>dsWOX10* line, when *WOX10* is downregulated upon 10 μ M 17 β -estradiol (17- β) treatment (middle and right panels), compared with mock-treated (DMSO) plant (left panel). (C) Quantitative representation of crown root (CR) number shows lesser and delayed CR formation is delayed upon 17- β treatment ($n=12$). Data are mean number \pm s.e.m. (D,E) Reduced growth of emerged CRs ($n=10$) and lateral roots (LRs) upon downregulation of *WOX10*. (F) Cumulative length of all CRs per 9-day-old plant plotted with s.e.m. (G) Root architecture upon ectopic overexpression of *WOX10* (right) compared with control (left). Number and growth of CRs and LRs were increased in the 14-day-old plant. (H) Dot plot for CR number in multiple 14-day-old *WOX10* overexpression lines (OE#3, OE#11 and OE#16) compared with the control plants. The bars represent mean \pm s.d., and each dot indicates individual data points. Sample size (n) is mentioned in panels B-D, F-H. Red arrows and arrowheads mark CR and LR, respectively, in B,D,E,G. PR, primary root. * $P \leq 0.05$; ** $P \leq 0.005$; *** $P \leq 0.001$; two-tailed unpaired Student's *t*-test. Scale bars: 1 cm.

Hofhuis et al., 2013; Kareem et al., 2015; Du and Scheres, 2017), we took an ectopic-expression-based approach to avoid the possible redundancy. We generated inducible *PLT2-GR* overexpression rice lines and analyzed effects of *PLT2* overexpression in root formation. Dex treatment of these lines resulted in high density lengthy LR formation from both PR and CRs, compared with the mock-treated plants (Fig. 6G; Fig. S10E,F, I; Fig. S11C). Similar dex treatment of wild-type rice plants did not display any such phenotypes (Fig. S10A-D; Fig. S11A).

Importantly, similar to wild-type plants, the CR number was not significantly affected in dex-treated multiple *PLT2-GR* lines compared with mock-treated lines (Fig. 6H; Fig. S10G-I). The RT-PCR analysis confirmed the expression of the *PLT2-GR* fusion gene in *PLT2-GR* lines (Fig. S11E). This observation indicates that *PLT2* has conserved function in regulating root-borne LRs but not in shoot-borne CR formation. However, our study cannot rule out whether *PLT2* has a redundant role in CR development with other PLT genes.

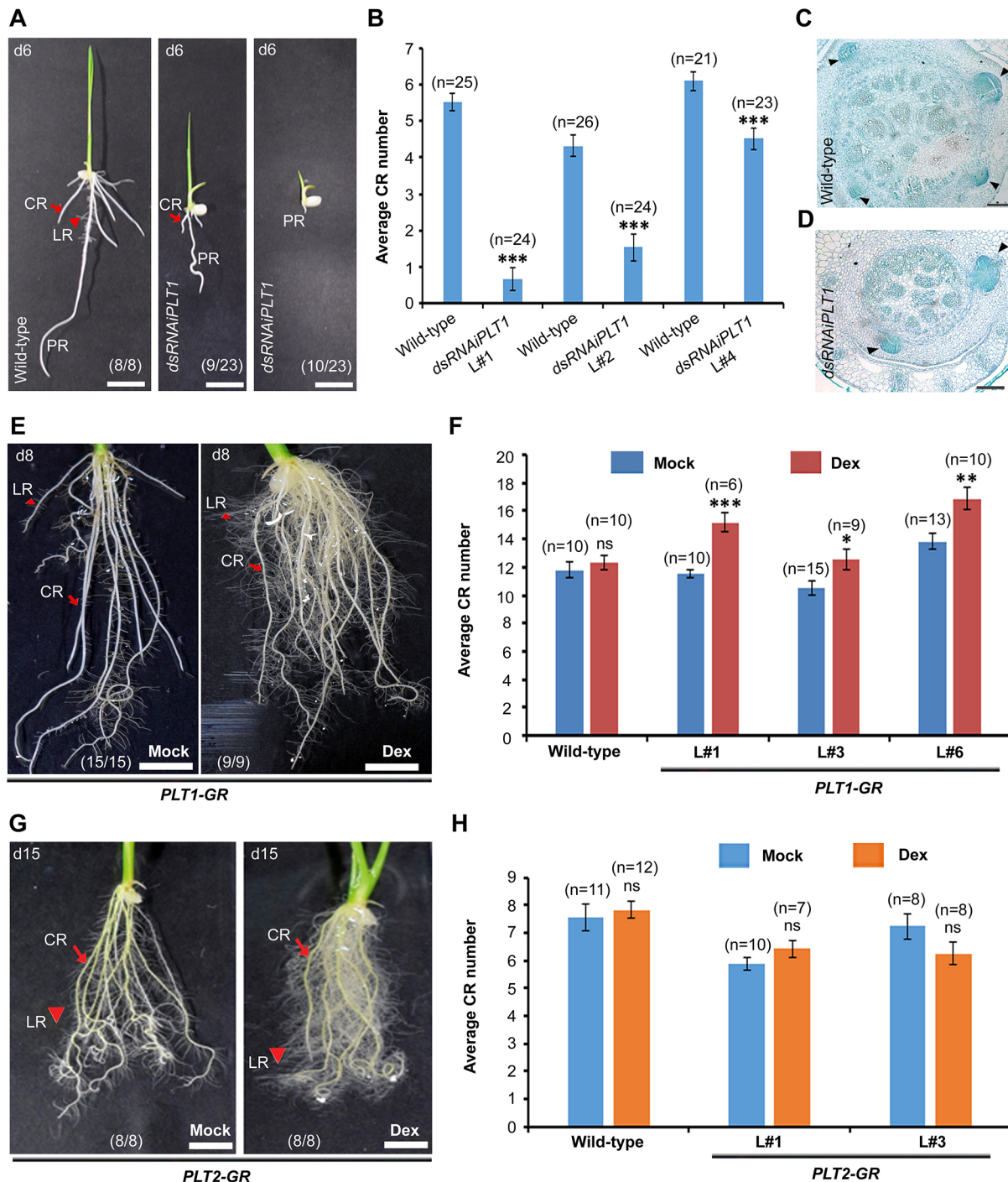


Fig. 6. Conserved and species-specific functions of rice PLT genes. (A) Root architecture phenotypic comparison of 6-day-old *PLT1* knockdown line (middle and right panels) with wild-type control plants (left panel). The length of all root-types i.e. primary root (PR), crown root (CR) and lateral root (LR) was greatly reduced in the *PLT1* downregulated line (*dsRNAiPLT1*). (B) Quantitative representation of CR number in 6-day-old wild-type and three independent *dsRNAiPLT1* knockdown lines. CR number is strongly reduced in these lines. Data are mean of CR number \pm s.e.m. (*** $P \leq 0.001$; two-tailed unpaired Student's *t*-test). (C,D) Cross-section of rice stem base from wild-type (C) and *dsRNAiPLT1* knock-down line (D), showing less CRP in the *PLT1* knockdown line. (E) Root architecture of 8-day-old *PLT1-GR* plants upon 5 μ M dexamethasone (Dex) treatment (right) compared with mock-treated plants (left). Number and length of CRs and LRs are increased in dex-treated plants. (F) Quantitative estimation confirms significantly increased CR number in 10-day-old three independent *PLT1-GR* overexpression lines upon dex-treatment but not in wild-type plants. Data are mean of CR number \pm s.e.m. (ns, not significant $P > 0.05$; * $P \leq 0.05$; ** $P \leq 0.005$; *** $P \leq 0.001$; two-tailed unpaired Student's *t*-test). (G) Root architecture comparison of 15-day-old *PLT2-GR* plants upon 10 μ M dex treatment. Data are mean of CR number in 7-day-old plants \pm s.e.m. in two independent lines (ns, not significant $P > 0.05$; two-tailed unpaired Student's *t*-test). Sample size (*n*) is mentioned in panels A,B,E-H. Red arrows and arrowheads mark CR and LR, respectively, in A,E,G. Scale bars: 100 μ m (C,D); 1 cm (A,E,G).

***PLT1* directly activates local auxin biosynthesis genes during rice CR development**

PLT genes regulate local auxin biosynthesis to control phyllotaxis and vascular regeneration by regulating the expression of YUCCA (YUC) genes in *Arabidopsis* (Pinon et al., 2013; Radhakrishnan et al., 2020). However, it remains unknown how the PLT genes regulate lateral root development in *Arabidopsis*. As our DR5-YFP localization studies indicate the necessity of a build-up of high auxin response, we asked whether rice PLT genes can contribute towards generating a high auxin response by activating local auxin biosynthesis genes. Interestingly, we observed reduced expression of *YUC1* and *YUC3* in *PLT1* knockdown lines compared with wild-type (Fig. 7A), suggesting the requirement of *PLT1* for upregulation of rice YUC genes. Next, to study whether *PLT1* is sufficient to induce *YUC1* and *YUC3* in the ectopic tissues, their expression level was analyzed in the leaf blade in dex-treated *PLT1-GR* plants. The expression of both of these genes was induced upon induction of *PLT1* overexpression (Fig. 7A), further validating that *PLT1* activates the expression of auxin biosynthesis genes.

To further investigate whether *PLT1* could directly activate the expression of YUC genes, we treated *PLT1-GR* plants with dex in the presence of the protein synthesis inhibitor cycloheximide (cyc). Dex treatment induced expression of *YUC1* and *YUC3* in presence of cyc (Fig. 7A), indicating that *PLT1* might activate YUC genes directly during CRP establishment. To further confirm that *PLT1*-mediated auxin biosynthesis is required for shoot-borne CR formation, we supplemented auxin (1-naphthaleneacetic acid; NAA) to rootless *dsRNAiPLT1* plants (Fig. 7B). Exogenous treatment of NAA induced rooting in these lines (Fig. 7C), to the extent of being similar to wild-type plants (Fig. 7C). These observations reinforce our notion that *PLT1* regulates rice root development by upregulating the expression of rice YUC genes.

The root outgrowth-promoting function of PLTs is conserved in *Arabidopsis*

As PLT genes in *Arabidopsis* set out LR outgrowth (Du and Scheres, 2017), we explored whether the function of rice PLTs is also conserved in *Arabidopsis*. Towards this, we expressed rice *PLT1* and *PLT2* in the lateral root primordia (LRP) of the *Arabidopsis* *plt3;plt5-2;plt7* triple mutant, defective in LRP outgrowth (Fig. 7D; Fig. S12). Strikingly, the LR outgrowth defect in the *plt3;plt5-2;plt7* triple mutant was rescued by *PLT1* when it was expressed in the *Arabidopsis* *PLT3* domain (Fig. 7D). Similarly, *PLT2* expression under the *Arabidopsis* *PLT5* promoter (*plt 3;5;7; AtPLT5::OsPLT2-YFP*) also rescued LR outgrowth in the triple mutant wherein, upon reconstitution, LR formation resembled the wild-type (Fig. S12A-D; Radhakrishnan et al., 2020). This result suggests that PLT-like genes have acquired a species-specific expression domain and the function of proteins is conserved, i.e. to promote root primordia irrespective of their developmental origin.

DISCUSSION

The origin of post-embryonic roots and their architecture is diverged across the plant species. In *Arabidopsis*, ARs and LR originate from the xylem pole pericycle cells of embryonically developed hypocotyl and PR, respectively (Scheres et al., 1994; Bellini et al., 2014). In tomato, LR and stem-borne ARs develop from pericycle and differentiated phloem cell, respectively (Omary et al., 2022). On the other hand, in grasses such as maize and rice, ARs/CRs develop from the innermost ground tissues of post-embryonically developed stem and LR originate from the

endodermal and pericycle cells located opposite to the protophloem of PR and CR (Itoh et al., 2005; Bellini et al., 2014). Thus, the developmental context of LR and CR in grasses is distinct from dicot species; however, only a handful of rice and maize mutants for AR defects have been identified. In this study, using genomics and reverse genetics, we uncover a stage-specific gene expression atlas of rice CRP and specific functions of key TFs in orchestrating fibrous root architecture in rice. This also provides datasets of TFs for future studies to uncover functional gene regulatory networks instrumental for grass-specific AR formation.

In grasses, CR development begins with an induction phase in which shoot cells adjacent to the vascular cylinder transdifferentiate into root founder cells that re-enter the cell cycle to establish CRP (Itoh et al., 2005; Guan et al., 2015; Hostetler et al., 2021). This shoot-to-root cell fate transition requires a reprogramming of the founder cells. Local auxin biosynthesis and polar auxin transport generate essential auxin maxima at the site of root primordia before their establishment in *Arabidopsis* (Benková et al., 2003; De Rybel et al., 2010). Consistently, we find a spatially localized auxin response at the site of shoot-borne CRP and during tissue differentiation in rice, suggesting that buildup of high auxin at the inception site of primordia is a prerequisite for their development and it is a conserved feature across the plant species (Omary et al., 2022). Our study provides a global gene expression landscape of genetic reprogramming during shoot-borne CRP initiation and outgrowth. Our findings reveal how the transcriptional state of genetic and epigenetic regulators in the heterogeneous cellular environment coordinate the initiation and the outgrowth of rice CRP from the stem tissues. Furthermore, our in-depth *in situ* transcript localization of various cell fate-determining factors uncover their timely reorganization during progressive CR development. Apart from CRs, maize develops another type of ARs (i.e. BRs). Although many common pathways are shared in the formation of BRs, CRs and LR (Li et al., 2011), there are also genes uniquely expressed in each root type (Stelpflug et al., 2016). Recently, a cluster of transition cells was isolated by single-cell profiling of tomato stem-borne root (SBR) primordia that was considered as progenitors for new SBR meristems. These cells were enriched with multiple root stem cell regulators including SHOOTBORNE ROOTLESS (SBRL), PLT, MAGPIE and SHORT ROOT genes (Omary et al., 2022). The rice homologs of these factors were enriched during CRP initiation, suggesting that irrespective of the developmental origin of ARs, a set of conserved regulators may be involved in cell fate transition across the plant species.

In *Arabidopsis*, *WOX11* and *WOX12* redundantly regulate *de novo* root organogenesis from detached leaf explants (Liu et al., 2014), but their role in regulating natural AR and LR formation are not well established. The rice genome includes three homologous genes, *WOX10*, *WOX11* and *WOX12*. *WOX11* activates emergence and growth of rice CRs (Zhao et al., 2009, 2015). Our study unveils a previously unrecognized role of *WOX10* in timely activation of CR formation and growth. The expression of *WOX10* has previously been reported to be induced by auxin signaling (Neogy et al., 2019). Here, we show an overlap between the auxin maxima and the onset of *WOX10* activation during CRP establishment. In addition, *WOX10* promotes growth of LR. Recently, *WOX10* was shown to positively affect LR diameter (Kawai et al., 2022). On the other hand, three PLT genes, *PLT3*, *PLT5* and *PLT7* redundantly regulate root-borne LR primordia outgrowth in *Arabidopsis* (Du and Scheres, 2017). Interestingly, unlike *Arabidopsis*, downregulation of a single rice PLT gene, *PLT1* is sufficient to impair grass-specific

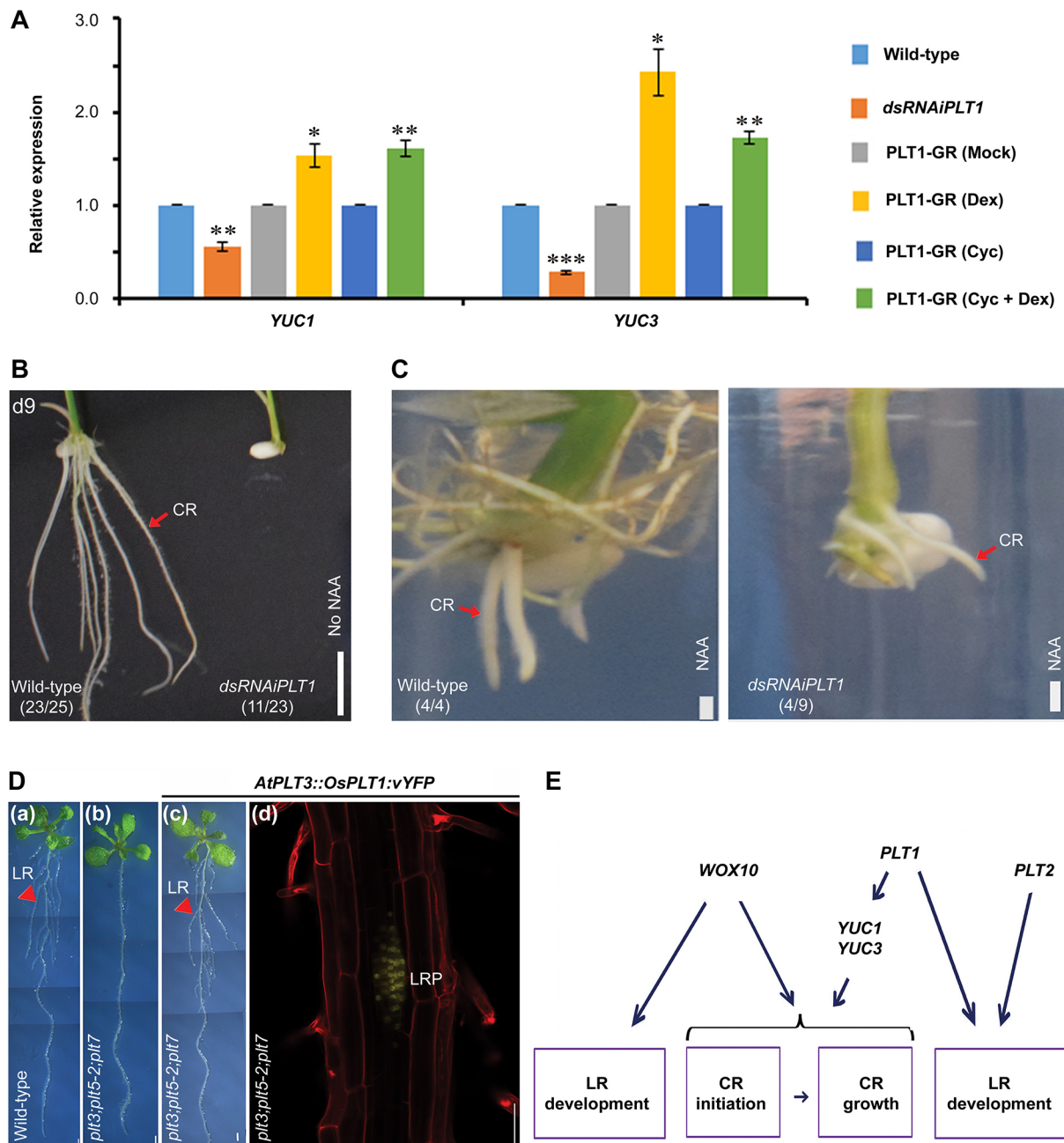


Fig. 7. Regulatory mechanism of *PLT1* function during crown root formation and its conserved role in root-borne lateral root development.

(A) *PLT1* promotes auxin biosynthesis. qRT-PCR analysis of auxin biosynthesis genes *YUC1* and *YUC3* in *PLT1* knockdown (*dsRNAiPLT1*) and overexpression (*PLT1-GR*) rice lines. Expression of YUC genes was reduced in *PLT1* downregulated lines. *PLT1* expression was induced in the leaf blades of the *PLT1-GR* line with dexamethasone (Dex) alone, and in presence of dexamethasone and protein synthesis inhibitor cycloheximide (Cyc) (dex+cyc). Ethanol (mock) and cycloheximide alone (Cyc) were used as background controls. Relative expression (fold change) is plotted \pm s.e.m. The *P*-value is calculated from four experiments (* $P \leq 0.05$; ** $P \leq 0.005$; *** $P \leq 0.001$; two-tailed unpaired Student's *t*-test). (B) Rootless phenotype of 9-day-old *dsRNAiPLT1* L#1 (right) compared with wild-type plant (left) in absence of auxin, 1-naphthaleneacetic acid (NAA). (C) Restoration of crown root (CR) formation in *dsRNAiPLT1* L#1 (right), similar to in control wild-type plants (left), after exogenous NAA treatment. Sample size (*n*) is mentioned in panels B and C. (D) Expression of *PLT1* in lateral root primordia (LRP) of *plt3;plt5-2;plt7* defective in LRP outgrowth rescued LRP outgrowth. Stereo images of 8-days post-germination wild-type plant (Da), *plt3;plt5-2;plt7* (Db) and *plt3;plt5-2;plt7;AtPLT3::OsPLT1::vYFP* (Dc). Confocal images showing expression of *PLT1::vYFP* in the LRP of *plt3;plt5-2;plt7;AtPLT3::OsPLT1::vYFP* (Dd). Red represents Propidium iodide staining. (E) Schematic depicting that *WOX10* and *PLTs* promote initiation and growth of post-embryonic roots. *PLT1* activates auxin biosynthesis genes *YUC1* and *YUC3*. Red arrows marks CRs; red arrowheads mark lateral roots (LR). Scale bars: 1 cm (B,C); 1 mm (Da-Dc); 50 μ m (Dd).

fibrous root architecture by modulating both root-borne LRs and shoot-borne CR development. Strikingly, we show that another rice *PLT* gene, *PLT2*, exclusively regulates LR development, whereas *PLT8* (*CRL5*) specifically controls CR development (Kitomi et al., 2011a). These studies provide deeper insights into how related

members of a large gene family have evolved to drive species-specific morphological diversity in root architecture. Although in *Arabidopsis* the mechanisms by which these *PLT* genes act in controlling LR and AR await future studies, we provide a possible molecular mechanism by which *PLT1* regulates rice root

architecture (Fig. 7E). We show that *PLT1* activates local auxin biosynthesis by upregulating the expression of YUC genes, which appears to be essential for CR formation (Fig. 7E). It will be interesting to explore whether orthologous WOX and PLT factors are functionally diverged between ARs (i.e. CRs and BRs) of the maize root system.

Functional conservation of rice root fate determinant is further evident from the rescue of root pericycle-originated LRPs outgrowth in *Arabidopsis* *plt3,5,7* mutants by delivering rice *PLT1* and *PLT2* in the LRP transcriptional domain. Our studies show that rice PLT genes have acquired species-specific function in regulating shoot-borne CR development while retaining their conserved role in root-borne LR formation. It is likely that conserved root-promoting factors such as PLTs have acquired species-specific function in the two evolutionarily diverged plant species, rice and *Arabidopsis*, largely by modulating the cis-regulatory sequences rather than by considerably changing the protein. Thus, it is tempting to speculate that the primary role of PLT genes in controlling organ primordia development is conserved across plant species. Future studies should reveal their functions in other grass species.

To conclude, this study provides genome-wide stage-specific transcriptional signatures at distinct developmental stages of CRP formation. It also reveals the early transcriptional onset of potential epigenetic modifiers and key cell fate-determining TFs required to reset the genetic program to re-activate cell division in competent cells to prime the initiation of CRP. We further report previously unrecognized functions of *WOX10* and two PLT genes (*PLT1* and *PLT2*) in controlling grass-specific fibrous root architecture in rice. These conserved cell fate determinants have acquired a species-specific function in regulating shoot-borne CR development, while retaining their conserved role in root-borne LR formation. Interestingly, PLT proteins have conserved roles in regulating root primordia outgrowth irrespective of their developmental origin. Our study provides datasets for generating coherent regulatory frameworks for revealing the underlying mechanistic diversity of root branching across the plant species (Lavarenne et al., 2020; Omary et al., 2022).

MATERIALS AND METHODS

Plant materials and treatments

O. sativa L. ssp. *indica* variety IR64 was used for LCM-seq and epigenetic analyses. Surface sterilized rice seeds were grown on ½ Murashige and Skoog (MS) medium with 0.3% phytagel (Sigma-Aldrich) with or without 3 mM sodium acetate (HiMedia), 20 µM 5-azacytidine (HiMedia) and 150 µM sodium butyrate (HiMedia). For inducible downregulation of *WOX10*, 10 µM 17β-estradiol (Sigma-Aldrich), dissolved in DMSO (Sigma-Aldrich), was used. For phenotyping *PLT1-GR* and *PLT2-GR* lines, 5 or 10 µM dex (Sigma-Aldrich) was used. For analyzing expression of *YUC1* and *YUC3* in *PLT1-GR*, leaf blades were treated with 10 µM dex (Sigma-Aldrich) and/or 10 µM cyc (Sigma-Aldrich), both dissolved in ethanol (Merck), for 6 h. Cyc treatments were started 30 min before the dex treatment in the samples that were treated with both reagents. For auxin treatment in *dsRNAiPLT1* lines, seedlings were grown on ½ MS medium for 9 days along with wild-type control. All old roots were cut and new roots were induced on ½ MS medium supplemented with 0.1 mg/l NAA (Sigma-Aldrich).

Laser capture microdissection

For LCM, 1 mm coleoptile base tissue from 6-day-old rice seedlings (var. IR-64) was harvested in Carnoy's fluid (ethanol: chloroform: acetic acid glacial; 6:3:1), infiltrated twice under mild vacuum and dehydrated using a graded ethanol series with xylene replacement. The tissue was embedded in Paraplast (Sigma-Aldrich) and cut into 8 µm thin sections using a RM2125 microtome (Leica Biosystems), which were then placed on PEN membrane slides (Carl-Zeiss). The CRP were micro-dissected on a PALM Microbeam

(Carl-Zeiss) and collected in RNA extraction buffer (Thermo Fisher Scientific).

RNA extraction, library preparation and RNA-seq

Total RNA from eleven initiating- and ten outgrowing-stage CRP for each replicate was isolated using ARCTURUS PicoPure RNA Isolation Kit (Thermo Fisher Scientific) according to the manufacturer's protocol. RNA was quantified on a 2100 Bioanalyzer using the RNA 6000 Pico Kit (Agilent Technologies). About 10–50 ng of the total RNA samples were depleted for ribosomal RNAs using Ribo-Zero rRNA Removal Kit (Illumina), followed by cDNA synthesis using SMART-Seq™ v4 Ultra™ Low input RNA Kit –v4 (Takara Bio) with 15-cycle cDNA amplification (Macrogen). RNA-seq libraries were synthesized and amplified for 15 enrichment cycles using TruSeq RNA Library Prep Kit v2 kit (Illumina). The quality control analysis of libraries was performed using the Agilent 2100 TapeStation System with a High Sensitivity D1000 Kit (Agilent Technologies). All LCM-seq libraries with a fragment size range of 285–382 bp were sequenced on the Nova Seq 6000 Platform (Illumina) by Macrogen.

RNA-seq data quality control analysis

The paired-end reads were mapped to the rice reference genome (MSU release 7) using STAR (Dobin et al., 2013) in two-pass mode. A gene count matrix was generated using quant mode-GeneCounts with rows corresponding to individual genes and columns corresponding to samples. The FPKM values were calculated from the gene counts, and the distribution of log₂ (FPKM) values was analyzed and shown in the box plot. Pearson's correlation coefficient (PCC) using log₂ (FPKM) values was calculated to assess the variability between biological replicates of each stage. The variability between experimental conditions was assessed using multidimensional scaling. Next, the log₂ (FPKM) values from each sample were projected to a two-dimensional scale to show the variability between biological replicates and different developmental stages.

Gene cluster analysis

For gene cluster and differential gene expression analysis, the RNA-seq data were analyzed following the pipeline used previously for LCM-seq data analysis (Harrop et al., 2016). For common gene expression pattern analysis, fuzzy c-means clustering was performed on RNA-seq data using Mfuzz (Kumar and Futschik, 2007). The gene count table was made homoscedastic using the variance-stabilizing transformation (VST) function in DESeq2 (Love et al., 2014). The biological replicates for each stage were collapsed using the geometric mean of the two values for each gene. After running fuzzy c-means clustering, a membership cutoff of 0.5 was used for assigning genes to individual clusters. The number of clusters was empirically determined from the top 30% of the most variable genes using principal component analysis (PCA) plots, minimum cluster centroid distance and normalized expression plots, with the number of clusters varying from 2 to 25 as in Harrop et al. (2016). The cluster-wise gene list (log₂ fold enrichment ≥1; *P* < 0.05) was used to perform Gene Ontology (GO) enrichment analysis using monocot PLAZA 4.5 workbench (<https://bioinformatics.psb.ugent.be/plaza/>).

Differential gene expression and GO analysis

The count matrix was used as input for differential expression analysis using DESeq2. Genes with an adjusted *P*-value (*q*-value) less than 0.05 and log₂ fold-change ≥1 or ≤−1 were considered as DEGs. Gene expression in different root zones was analyzed with the CoNekT database (<https://conekt.sbs.ntu.edu.sg>) and a heatmap was generated using the Heatmapper tool (<http://heatmapper.ca/expression/>). GO enrichment analysis for DEGs was performed using BiNGO plug-in of Cytoscape (version 3.3.0) with a *P*-value ≤0.05. GO enrichment of different sets of DEGs was further used to generate a comparative enrichment map via Cytoscape.

Real-time PCR

Total RNA from rice tissues was extracted using RNeasy Plant Mini Kit (Qiagen) followed by elimination of DNA using on-column DNase

(Qiagen) according to the manufacturer's protocol. The cDNA synthesis and qRT-PCR were performed as previously described (Neogy et al., 2019) using the iScript cDNA synthesis kit and iTaq Universal SYBR Green Supermix (Bio-Rad Laboratories). Rice *UBQ5*-normalized $\Delta\Delta C_t$ was used to calculate relative fold change in the gene expression. A list of primers is provided as Table S8. For the statistical significance of fold-change, *P*-values were calculated using a two-tailed, unpaired Student's *t*-test from at least three experiments.

RNA in situ hybridization

For preparing antisense DIG-UTP-labeled riboprobes, 121 bp of *TRX1*, 132 bp of *SWIB/MDM2*, 150 bp of *ERF3*, 186 bp of *ARF16*, 170 bp of *HOX1*, 526 bp of *WOX10* and 152 bp of *PLT2* gene-specific fragments were cloned in pBluescript SK+ (antisense), linearized with EcoRI and transcribed with T7 RNA Polymerase (Sigma-Aldrich). Their sense clones in pBluescript SK+ with EcoRI/T7 RNA polymerase were used to generate sense probes. The 152 bp of *PLT2*, 193 bp of *RR24* and 134 bp of *ATXR6* gene-specific fragments were cloned in pBS SK+ (antisense), EcoRI/T7 RNA polymerase and HindIII/T3 RNA polymerase (New England Biolabs) generated antisense and sense probes, respectively. For YFP antisense probe, 609 bp of YFP fragment was cloned in pBS SK+ (antisense) and transcribed with EcoRI/T7 RNA polymerase. A gene-specific 617 bp region of *PLT1* cloned in pBS SK+ (sense) was transcribed with T3 RNA polymerase for antisense and with T7 RNA polymerase for sense probes. Probes for YFP, *WOX10* and *PLT1* were hydrolyzed to ~100–120 bp before use. Hybridization and detection were performed on 8 μ m paraffin-embedded cross-sections of 6-day-old rice stem base as previously described studies (Yadav et al., 2007; Neogy et al., 2019, 2021).

Immunohistochemistry

For immunohistochemistry, 8 μ m cross-sections of rice stem base were treated for antigen retrieval in antigen retrieval buffer (10 mM Tris, 1 mM EDTA, pH 9.0). Slides were blocked with 1% bovine serum albumin (Sigma-Aldrich) in 1 \times TBST (20 mM Tris, 150 mM NaCl, 0.1% w/v Tween-20) and incubated with anti-GFP primary antibody raised in mouse [a gift from Dr Prabhat Kumar Mandal, Indian Institute of Technology (IIT) Roorkee, India] at 1:500 dilution for 10–12 h. Slides were washed with 1 \times TBST and incubated with HRP-conjugated anti-mouse (goat) IgG secondary antibody (115-035-174, Jackson ImmunoResearch Laboratories) at 1:3000. Color detection was carried out using 3,3'-diaminobenzidine (11718096001, Roche/Sigma-Aldrich) as a substrate. Sections were counterstained with hematoxylin (HiMedia), dehydrated with graded ethanol, cleared with xylene (HiMedia) and mounted in DPX (HiMedia).

Plasmid construction and generating transgenic line

For generating the auxin promoter-reporter construct, DR5rev::erYFP-nosT fragment was PCR amplified on plasmid pHm-DR5rev::erYFP-nosT vector (a gift from Dr Ari Pekka Mähönen, University of Helsinki, Finland) and was cloned into a pCambia1390 backbone as pDR5rev::erYFP for rice transformation. For the *WOX10* downregulation construct, a 526 bp gene-specific fragment was used to generate an inverted repeat RNAi hairpin loop. For inducible expression of the RNAi construct, the pUN vector [a gift from Dr Usha Vijayraghavan, Indian Institute of Science (IISc), Bangalore, India] was modified by subcloning the XVE fragment from p1R4-ML:XVE (obtained from Dr Ari Pekka Mähönen) under the maize Ubiquitin promoter. The RNAi inverted repeat was cloned downstream of XVE to generate *pUbi::XVE>dsWOX10*. For ectopic overexpression, the full-length coding DNA sequence of *WOX10* was cloned in pUN under the maize Ubiquitin promoter to generate *pUbi::WOX10* (Prasad et al., 2005). For generating the *dsRNAiPLT1* construct, the gene-specific fragment of *PLT1* (979 bp) was used to generate an RNAi hairpin loop and was cloned in the pUN vector. For generating the *PLT1-GR* and *PLT2-GR* constructs, full-length open reading frames of *PLT1* (*LOC_Os04g55970.2*) and *PLT2* (*LOC_Os06g44750.1*) without a stop codon were PCR amplified and cloned in the pUGN vector (a gift from Dr Usha Vijayraghavan) for translational fusion with the rat GR (Prasad et al., 2005). These constructs were mobilized to *Agrobacterium tumefaciens* LBA4404 and used to raise transgenic rice lines in the *O. sativa* L. ssp. *japonica* cultivar TP309 as

described by Toki et al. (2006). For complementation of *Arabidopsis* *plt* mutants, *PLT1* (*LOC_Os04g55970.2*) was amplified from genomic DNA extracted from rice leaf tissues. The *PLT1* gene was cloned under the *Arabidopsis* *PLT3* promoter (7.7 Kb) and tagged with *vYFP* (Radhakrishnan et al., 2020). Similarly, the *PLT2* (*LOC_Os06g44750.1*) gene tagged with *vYFP* and driven by the *Arabidopsis* *PLT5* promoter (5.0 Kb) was cloned (Radhakrishnan et al., 2020). The constructs for *Arabidopsis* transformation were cloned using the Multisite gateway recombination cloning system (Invitrogen) using pCambia 1300 destination vector. These constructs were electroporated into C58 *Agrobacterium* and transformed into *Arabidopsis* *plt3;plt5-2;plt7* mutant plants using the floral dip method (Clough and Bent, 1998).

Rice phenotyping and histology

For studying the CR phenotype of *WOX10* downregulation, seeds were grown on solid 1/2 MS medium with 1% sucrose supplemented with 10 μ M 17 β -estradiol for 4 days and then 17 β -estradiol treatment in liquid 1/2 MS medium for the remaining period. For *WOX10* overexpression and *PLT1* constitutive downregulation, the seeds were grown on solid 1/2 MS medium with 1% sucrose before imaging. *PLT1-GR* and *PLT2-GR* plants were treated with 5 or 10 μ M dex on 1/2 MS medium solidified with phytigel (Sigma-Aldrich). The CR number was counted in both wild-type and multiple transgenic lines in 2–3 replicates. For statistical significance of the CR number, *P*-values were calculated using a two-tailed, unpaired Student's *t*-test using the Microsoft Excel tool, Two-sample Assuming Unequal Variances. For analyzing LR phenotypes, PRs and CRs were dissected and imaged. For histology, 4% paraformaldehyde-fixed stem bases were embedded in Paraplast (Sigma-Aldrich), cut into 10 μ m thin sections using an HM 325 rotary microtome (Thermo Fisher Scientific) and stained with Toluidine Blue (Sisco Research Laboratories) for imaging using an Axio Scope A1 light microscope (Carl-Zeiss).

Phylogenetic analysis

For constructing the phylogenetic tree, the protein sequences of rice and *Arabidopsis* WOX homologs from the intermediate clade was taken. The *Arabidopsis* protein sequences were retrieved from The Arabidopsis Information Resource (TAIR; <http://www.arabidopsis.org>) and rice protein sequences were retrieved from the Rice Genome Annotation Project (RGAP; <http://rice.uga.edu>). The neighbor-joining phylogenetic tree was constructed using Mega 7 software with default parameters.

Acknowledgements

We thank Dr Harsh Chauhan, IIT Roorkee, for his input on the project. Dr Deepak Sharma, IIT Roorkee, and Bencos Research Solutions, India, are acknowledged for the initial help in RNA-seq data analysis. The anti-GFP antibody for immunohistochemistry was gifted by Dr Prabhat Kumar Mandal, IIT Roorkee, India. Plasmids pHm-DR5rev::erYFP-nosT and p1R4-ML-XVE were kindly provided by Dr Ari Pekka Mähönen, University of Helsinki, Finland. Dr Usha Vijayraghavan, Indian Institute of Science, Bangalore, India, kindly provided the plasmids pUN and pUGN. Manoj Yadav, Ashish Kumar and Sonia Choudhary are acknowledged for their support in growing plants. Dr Leena Yadav and Dr Kiran Ambatipudi, IIT Roorkee, are acknowledged for providing critical comments on the manuscript.

Competing interests

The authors declare no competing or financial interests.

Author contributions

Conceptualization: K.P., S.R.Y.; Methodology: T.G., Z.S., K.C., K.K.K.M., V.V., K.P., M.J., S.R.Y.; Software: A.K.D., R.S.S., M.J.; Validation: T.G., Z.S., K.C., K.K.K.M., A.K.D., V.V., H.S.; Formal analysis: T.G., Z.S., K.C., K.K.K.M., A.K.D., H.S., R.S.S.; Investigation: T.G., Z.S., K.C., K.K.K.M., V.V., H.S.; Resources: K.P., S.R.Y.; Data curation: T.G., A.K.D., R.S.S., M.J., S.R.Y.; Writing - original draft: K.P., S.R.Y.; Writing - review & editing: T.G., Z.S., D.S., K.P., M.J., S.R.Y.; Visualization: T.G., Z.S., K.C., K.K.K.M., V.V., H.S.; Supervision: K.P., M.J., D.S., D.C., S.R.Y.; Project administration: S.R.Y.; Funding acquisition: D.S., K.P., M.J., S.R.Y.

Funding

S.R.Y. acknowledges financial support from the Department of Biotechnology, Ministry of Science and Technology, India (DBT) (grant BT/PR13488/BPA/118/105/2015). M.J. received the Tata Innovation Fellowship from the DBT. K.P.

acknowledges grants from the DBT (grant BT/PR12394/AGIII/103/891/2014) and Science and Engineering Research Board (grant EMR/2017/002503/PS). We acknowledge the Indian Institute of Technology Roorkee for providing fellowships to T.G., Z.S. and K.K.K.M., the University Grants Commission for fellowships to K.C. and H.S., the Indian Council of Medical Research for a fellowship to A.K.D. and the Council of Scientific and Industrial Research, India a fellowship to V.V.

Data availability

The sequence datasets are deposited to the GEO database under series accession number GSE185198.

References

- Aida, M., Beis, D., Heidstra, R., Willemsen, V., Blilou, I., Galinha, C., Nussaume, L., Noh, Y.-S., Amasino, R. and Scheres, B. (2004). The PLETHORA genes mediate patterning of the Arabidopsis root stem cell niche. *Cell* **119**, 109-120. doi:10.1016/j.cell.2004.09.018
- Atkinson, J. A., Rasmussen, A., Traini, R., Voß, U., Sturrock, C., Mooney, S. J., Wells, D. M. and Bennett, M. J. (2014). Branching out in roots: uncovering form, function, and regulation. *Plant Physiol.* **166**, 538-550. doi:10.1104/pp.114.245423
- Bellini, C., Pacurac, D. I. and Perrone, I. (2014). Adventitious roots and lateral roots: similarities and differences. *Annu. Rev. Plant Biol.* **65**, 639-666. doi:10.1146/annurev-arplant-050213-035645
- Benková, E., Michniewicz, M., Sauer, M., Teichmann, T., Seifertová, D., Jürgens, G. and Friml, J. (2003). Local, efflux-dependent auxin gradients as a common module for plant organ formation. *Cell* **115**, 591-602. doi:10.1016/s0092-8674(03)00924-3
- Clough, S. J. and Bent, A. F. (1998). Floral dip: a simplified method for Agrobacterium-mediated transformation of Arabidopsis thaliana. *Plant J.* **16**, 735-743. doi:10.1046/j.1365-313x.1998.00343.x
- Coudert, Y., Périn, C., Courtois, B., Khong, N. G. and Gantet, P. (2010). Genetic control of root development in rice, the model cereal. *Trends Plant Sci.* **15**, 219-226. doi:10.1016/j.tplants.2010.01.008
- De Rybel, B., Vassileva, V., Parizot, B., Demeulenaere, M., Grunewald, W., Audenaert, D., Van Campenhout, J., Overvoorde, P., Jansen, L., Vanneste, S., et al. (2010). A novel Aux/IAA28 signaling cascade activates GATA23-dependent specification of lateral root founder cell identity. *Curr. Biol.* **20**, 1697-1706. doi:10.1016/j.cub.2010.09.007
- Dobin, A., Davis, C. A., Schlesinger, F., Drenkow, J., Zaleski, C., Jha, S., Batut, P., Chaisson, M. and Gingeras, T. R. (2013). STAR: ultrafast universal RNA-seq aligner. *Bioinformatics* **29**, 15-21. doi:10.1093/bioinformatics/bts635
- Du, Y. and Scheres, B. (2017). PLETHORA transcription factors orchestrate de novo organ patterning during Arabidopsis lateral root outgrowth. *Proc. Natl. Acad. Sci. USA* **114**, 11709-11714. doi:10.1073/pnas.1714410114
- Dubrovsky, J. G., Sauer, M., Napsucially-Mendivil, S., Ivanchenko, M. G., Friml, J., Shishkova, S., Celenza, J. and Benková, E. (2008). Auxin acts as a local morphogenetic trigger to specify lateral root founder cells. *Proc. Natl. Acad. Sci. USA* **105**, 8790-8794. doi:10.1073/pnas.0712307105
- Galinha, C., Hoffhuis, H., Luijten, M., Willemsen, V., Blilou, I., Heidstra, R. and Scheres, B. (2007). PLETHORA proteins as dose-dependent master regulators of Arabidopsis root development. *Nature* **449**, 1053-1057. doi:10.1038/nature06206
- Guan, L., Murphy, A. S., Peer, W. A., Gan, L., Li, Y. and Cheng, Z. M. (2015). Physiological and molecular regulation of adventitious root formation. *Crit. Rev. Plant Sci.* **34**, 506-521. doi:10.1080/07352689.2015.1090831
- Harrop, T. W. R., Ud Din, I., Gregis, V., Osnato, M., Jouannic, S., Adam, H. and Kater, M. M. (2016). Gene expression profiling of reproductive meristem types in early rice inflorescences by laser microdissection. *Plant J.* **86**, 75-88. doi:10.1111/tpl.13147
- Hetz, W., Hochholdinger, F., Schwall, M. and Feix, G. (1996). Isolation and characterization of rts, a maize mutant deficient in the formation of nodal roots. *Plant J.* **10**, 845-857. doi:10.1046/j.1365-313X.1196.10050845.x
- Hochholdinger, F., Woll, K., Sauer, M. and Dembinsky, D. (2004). Genetic dissection of root formation in maize (Zea mays) reveals root-type specific developmental programmes. *Ann. Bot.* **93**, 359-368. doi:10.1093/aob/mch056
- Hochholdinger, F., Yu, P. and Marcon, C. (2018). Genetic control of root system development in Maize. *Trends Plant Sci.* **23**, 79-88. doi:10.1016/j.tplants.2017.10.004
- Hoffhuis, H., Laskowski, M., Du, Y., Prasad, K., Grigg, S., Pinon, V. and Scheres, B. (2013). Phyllotaxis and rhizotaxis in Arabidopsis are modified by three plethra transcription factors. *Curr. Biol.* **23**, 956-962. doi:10.1016/j.cub.2013.04.048
- Hostetler, A. N., Khangura, R. S., Dilkes, B. P. and Sparks, E. E. (2021). Bracing for sustainable agriculture: the development and function of brace roots in members of Poaceae. *Curr. Opin. Plant Biol.* **59**, 101985. doi:10.1016/j.pbi.2020.101985
- Inukai, Y., Sakamoto, T., Ueguchi-Tanaka, M., Shibata, Y., Gomi, K., Umemura, I., Hasegawa, Y., Ashikari, M., Kitano, H. and Matsuoka, M. (2005). Crown rootless1, which is essential for crown root formation in rice, is a target of an Auxin Response Factor in auxin signaling. *Plant Cell* **17**, 1387-1396. doi:10.1105/tpc.105.030981
- Itoh, J.-I., Nonomura, K.-I., Ikeda, K., Yamaki, S., Inukai, Y., Yamagishi, H., Kitano, H. and Nagato, Y. (2005). Rice plant development: from zygote to spikelet. *Plant Cell Physiol.* **46**, 23-47. doi:10.1093/pcp/pci501
- Jégu, T., Latrasse, D., Delarue, M., Hirt, H., Domenichini, S., Ariel, F., Crespi, M., Bergounioux, C., Raynaud, C. and Benhamed, M. (2014). The BAF60 subunit of the SWI/SNF chromatin-remodeling complex directly controls the formation of a gene loop at FLOWERING LOCUS C in Arabidopsis. *Plant Cell* **26**, 538-551. doi:10.1105/tpc.113.114454
- Kareem, A., Durgaprasad, K., Sugimoto, K., Du, Y., Pulianmackal, A. J., Trivedi, Z. B., Abhayadev, P. V., Pinon, V., Meyerowitz, E. M., Scheres, B., et al. (2015). PLETHORA genes control regeneration by a two-step mechanism. *Curr. Biol.* **25**, 1017-1030. doi:10.1016/j.cub.2015.02.022
- Kawai, T., Shibata, K., Akahoshi, R., Nishiuchi, S., Takahashi, H., Nakazono, M., Kojima, T., Nosaka-Takahashi, M., Sato, Y., Toyoda, A., et al. (2022). WUSCHEL-related homeobox family genes in rice control lateral root primordium size. *Proc. Natl. Acad. Sci. USA* **119**, e2101846119. doi:10.1073/pnas.2101846119
- Kitomi, Y., Ito, H., Hobo, T., Aya, K., Kitano, H. and Inukai, Y. (2011a). The auxin responsive AP2/ERF transcription factor CROWN ROOTLESS5 is involved in crown root initiation in rice through the induction of OsRR1, a type-A response regulator of cytokinin signaling. *Plant J.* **67**, 472-484. doi:10.1111/j.1365-313X.2011.04610.x
- Kitomi, Y., Kitano, H. and Inukai, Y. (2011b). Molecular mechanism of crown root initiation and the different mechanisms between crown root and radicle in rice. *Plant Signal Behav.* **6**, 1270-1278. doi:10.416/psb.6.9.16787
- Kumar, L. and Futschik, M. E. (2007). Mfuzz: a software package for soft clustering of microarray data. *Bioinformatics* **23**, 5-7. doi:10.1093/bioinformatics/btm02005
- Lavarenne, J., Gonin, M., Champion, A., Javelle, M., Adam, H., Rouster, J., Conejero, G., Lartaud, M., Verdel, J.-L., Laplace, L., et al. (2020). Transcriptome profiling of laser-captured crown root primordia reveals new pathways activated during early stages of crown root formation in rice. *PLoS One* **15**, e0238736. doi:10.1371/journal.pone.0238736
- Lavenus, J., Goh, T., Roberts, I., Guyomarc'h, S., Lucas, M., De Smet, I., Fukaki, H., Beeckman, T., Bennett, M. and Laplace, L. (2013). Lateral root development in Arabidopsis: fifty shades of auxin. *Trends Plant Sci.* **18**, 450-458. doi:10.1016/j.tplants.2013.04.006
- Li, S.-W. (2021). Molecular bases for the regulation of adventitious root generation in plants. *Front. Plant Sci.* **12**, 614072. doi:10.3389/fpls.2021.614072
- Li, P. and Xue, H. (2011). Structural characterization and expression pattern analysis of the rice PLT gene family. *Acta Biochim. Biophys. Sin.* **43**, 688-697. doi:10.1093/abbs/gmr068
- Li, Y.-J., Fu, Y.-R., Huang, J.-G., Wu, C.-A. and Zheng, C.-C. (2011). Transcript profiling during the early development of the maize brace root via Solexa sequencing. *FEBS J.* **278**, 156-166. doi:10.1111/j.1742-4658.2010.07941.x
- Li, J., Chen, F., Li, Y., Li, P., Wang, Y., Mi, G. and Yuan, L. (2019). ZmRAP2.7, an AP2 transcription factor, is involved in maize brace roots development. *Front. Plant Sci.* **10**, 820. doi:10.3389/fpls.2019.00820
- Liu, H., Wang, S., Yu, X., Yu, J., He, X., Zhang, S., Shou, H. and Wu, P. (2005). ARL1, a LOB-domain protein required for adventitious root formation in rice. *Plant J.* **43**, 47-56. doi:10.1111/j.1365-313X.2005.02434.x
- Liu, J., Sheng, L., Xu, Y., Li, J., Yang, Z., Huang, H. and Xu, L. (2014). WOX11 and 12 are involved in the first-step cell fate transition during de novo root organogenesis in Arabidopsis. *Plant Cell* **26**, 1081-1093. doi:10.1105/tpc.114.122887
- López-González, L., Mouriz, A., Narro-Diego, L., Bustos, R., Martínez-Zapater, J. M., Jarillo, J. A. and Piñeiro, M. (2014). Chromatin-dependent repression of the Arabidopsis floral integrator genes involves plant specific PHD-containing proteins. *Plant Cell* **26**, 3922-3938. doi:10.1105/tpc.114.130781
- Love, M. I., Huber, W. and Anders, S. (2014). Moderated estimation of fold change and dispersion for RNA-seq data with DESeq2. *Genome Biol.* **15**, 550. doi:10.1186/s13059-014-0550-8
- Luong, A. M., Adam, H., Gauron, C., Affortit, P., Ntakirutimana, F., Khong, N. G., Le, Q. H., Le, T. N., Fournel, M., Lebrun, M., et al. (2021). Functional diversification of euANT/PLT genes in oryza sativa panicle architecture determination. *Front. Plant Sci.* **12**, 1383. doi:10.3389/fpls.2021.692955
- Meng, F., Xiang, D., Zhu, J., Li, Y. and Mao, C. (2019). Molecular mechanisms of root development in rice. *Rice* **12**, 1. doi:10.1186/s12284-018-0262-x
- Mouriz, A., López-González, L., Jarillo, J. A. and Piñeiro, M. (2015). PHDs govern plant development. *Plant Signal Behav.* **10**, e993253. doi:10.4161/15592324.2014.993253
- Neogy, A., Garg, T., Kumar, A., Dwivedi, A. K., Singh, H., Singh, U., Singh, Z., Prasad, K., Jain, M. and Yadav, S. R. (2019). Genome-wide transcript profiling reveals an auxin-responsive transcription factor, OsAP2/ERF-40, Promoting Rice Adventitious Root Development. *Plant Cell Physiol.* **60**, 2343-2355. doi:10.1093/pcp/pcz132
- Neogy, A., Singh, Z., Mushahary, K. K. K. and Yadav, S. R. (2021). Dynamic cytokinin signaling and function of auxin in cytokinin responsive domains during rice crown root development. *Plant Cell Rep.* **40**, 1367-1375. doi:10.1007/s00299-020-02618-9

- Okushima, Y., Fukaki, H., Onoda, M., Theologis, A. and Tasaka, M. (2007). ARF7 and ARF19 regulate lateral root formation via direct activation of LBD/ASL genes in Arabidopsis. *Plant Cell* **19**, 118–130. doi:10.1105/tpc.106.047761
- Omary, M., Gil-Yarom, N., Yahav, C., Steiner, E., Hendelman, A. and Efroni, I. (2022). A conserved superlocus regulates above- and belowground root initiation. *Science* **375**, eabf4368. doi:10.1126/science.abf4368
- Orman-Ligeza, B., Parizot, B., Gantet, P. P., Beeckman, T., Bennett, M. J. and Draye, X. (2013). Post-embryonic root organogenesis in cereals: Branching out from model plants. *Trends Plant Sci.* **18**, 459–467. doi:10.1016-j.tplants.201304.010
- Pinon, V., Prasad, K., Grigg, S. P., Sanchez-Perez, G. F. and Scheres, B. (2013). Local auxin biosynthesis regulation by PLETHORA transcription factors controls phyllotaxis in Arabidopsis. *Proc. Natl. Acad. Sci. USA* **110**, 1107–1112. doi:10.1073/pnas.1213497110
- Prasad, K., Parameswaran, S. and Vijayraghavan, U. (2005). OsMADS1, a rice MADS-box factor, controls differentiation of specific cell types in the lemma and palea and is an early-acting regulator of inner floral organs. *Plant J.* **43**, 915–928. doi:10.1111/j.1365-313X.2005.02504.x
- Prasad, K., Grigg, S. P., Barkoulas, M., Yadav, R. K., Sanchez-Perez, G., Pinon, V., Bilou, I., Hofhuis, H., Dhonukshe, P., Galinha, C., et al. (2011). Arabidopsis PLETHORA transcription factors control phyllotaxis. *Curr. Biol.* **21**, 1123–1128. doi:10.1016/j.cub.2011.05.009
- Radhakrishnan, D., Shanmukhan, A. P., Kareem, A., Aiyaz, M., Varappambathu, V., Toms, A., Kerstens, M., Valsakumar, D., Landge, A. N., Shaji, A., et al. (2020). A coherent feed-forward loop drives vascular regeneration in damaged aerial organs of plants growing in a normal developmental context. *Development* **147**, dev185710. doi:10.1242/dev.185710
- Scheres, B., Wolkenfelt, H., Willemsen, V., Terlouw, M., Lawson, E., Dean, C. and Weisbeek, P. (1994). Embryonic origin of the Arabidopsis primary root and root meristem initials. *Development* **120**, 2475–2487. doi:10.1242/dev.120.9.2475
- Steffens, B. and Rasmussen, A. (2016). The physiology of adventitious roots. *Plant Physiol.* **170**, 603–617. doi:10.1104/pp.15.01360
- Stelplflug, S. C., Sekhon, R. S., Vaillancourt, B., Hirsch, C. N., Buell, C. R., de Leon, N. and Kaeppler, S. M. (2016). An expanded maize gene expression atlas based on RNA sequencing and its use to explore root development. *Plant Genome* **9**, plantgenome2015.04.0025. doi:10.3835/plantgenome2015.04.0025
- Toki, S., Hara, N., Ono, K., Onodera, H., Tagiri, A., Oka, S. and Tanaka, H. (2006). Early infection of scutellum tissue with Agrobacterium allows high-speed transformation of rice. *Plant J.* **47**, 969–976. doi:10.1111/j.1365-313X.2006.02836.x
- Yadav, S. R., Prasad, K. and Vijayraghavan, U. (2007). Divergent regulatory OsMADS2 functions control size, shape and differentiation of the highly derived rice floret second-whorl organ. *Genetics* **176**, 283–294. doi:10.1534/genetics.107.071746
- Yang, J., Yuan, Z., Meng, Q., Huang, G., Périn, C., Bureau, C., Meunier, A.-C., Ingouff, M., Bennett, M. J., Liang, W., et al. (2017). Dynamic regulation of auxin response during rice development revealed by newly established hormone biosensor markers. *Front. Plant Sci.* **8**, 256. doi:10.3389/fpls.2017.00256
- Zhao, Y., Hu, Y., Dai, M., Huang, L. and Zhou, D. X. (2009). The WUSCHEL-related homeobox gene WOX11 is required to activate shoot-borne crown root development in rice. *Plant Cell* **21**, 736–748. doi:10.1105/tpc.108.061655
- Zhao, Y., Cheng, S., Song, Y., Huang, Y., Zhou, S., Liu, S. and Zhou, D. X. (2015). The interaction between rice ERF3 and WOX11 promotes crown root development by regulating gene expression involved in cytokinin signaling. *Plant Cell* **27**, 2469–2483. doi:10.1105/tpc.15.00227



YFP (as)/wild-type

Fig. S1. Negative control for auxin response analysis. RNA *in situ* hybridization using antisense YFP riboprobes on the cross section of stem base of 6-day old wild-type plant as a control. Red arrows mark crown root primordia (CRP). Bars= 100 μm.

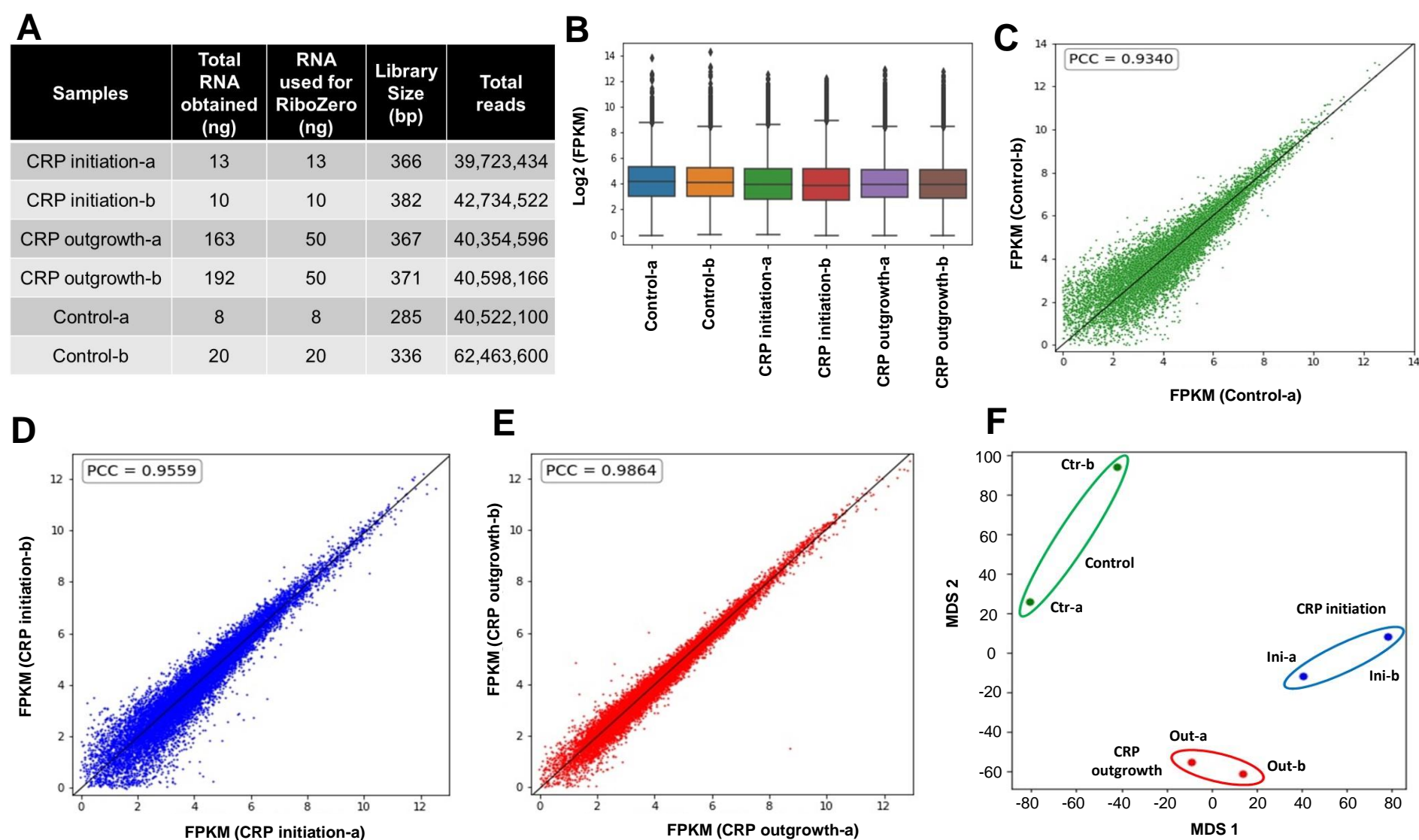


Fig. S2. LCM-seq data quality control. (A) Data QC of library and RNA seq data. RNA quantity, library size and total reads are given in the table. (B) Box plot showing the range of log₂ FPKM values for the replicates. (C-E) Scatter plots depicting the Pearson's correlation coefficient (PCC) values between log₂ transformed FPKM values of two replicates of control (C), CRP initiation (D), and CRP outgrowth (E). PCC values (0.93-0.99) indicate high correlation between the replicates for each stage. (F) Multidimensional scaling plots of all replicates of control, CRP initiation and CRP outgrowth, showing low divergence between the replicates.

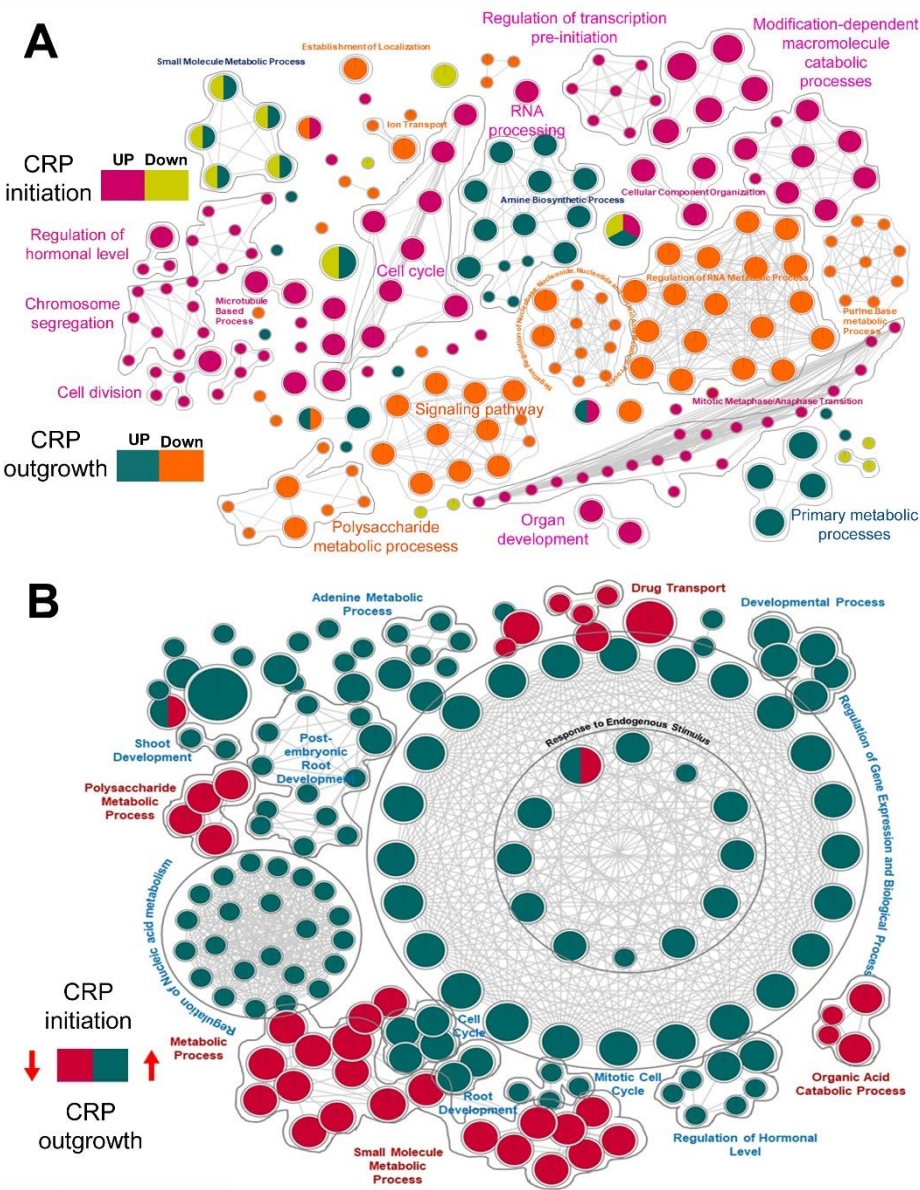


Fig. S3. Gene ontology analysis of DEGs. (A) GO terms associated with genes specifically de-regulated during CRP initiation and outgrowth. (B) GO analysis of DEGs when CRP progress from initiation to outgrowth stage.

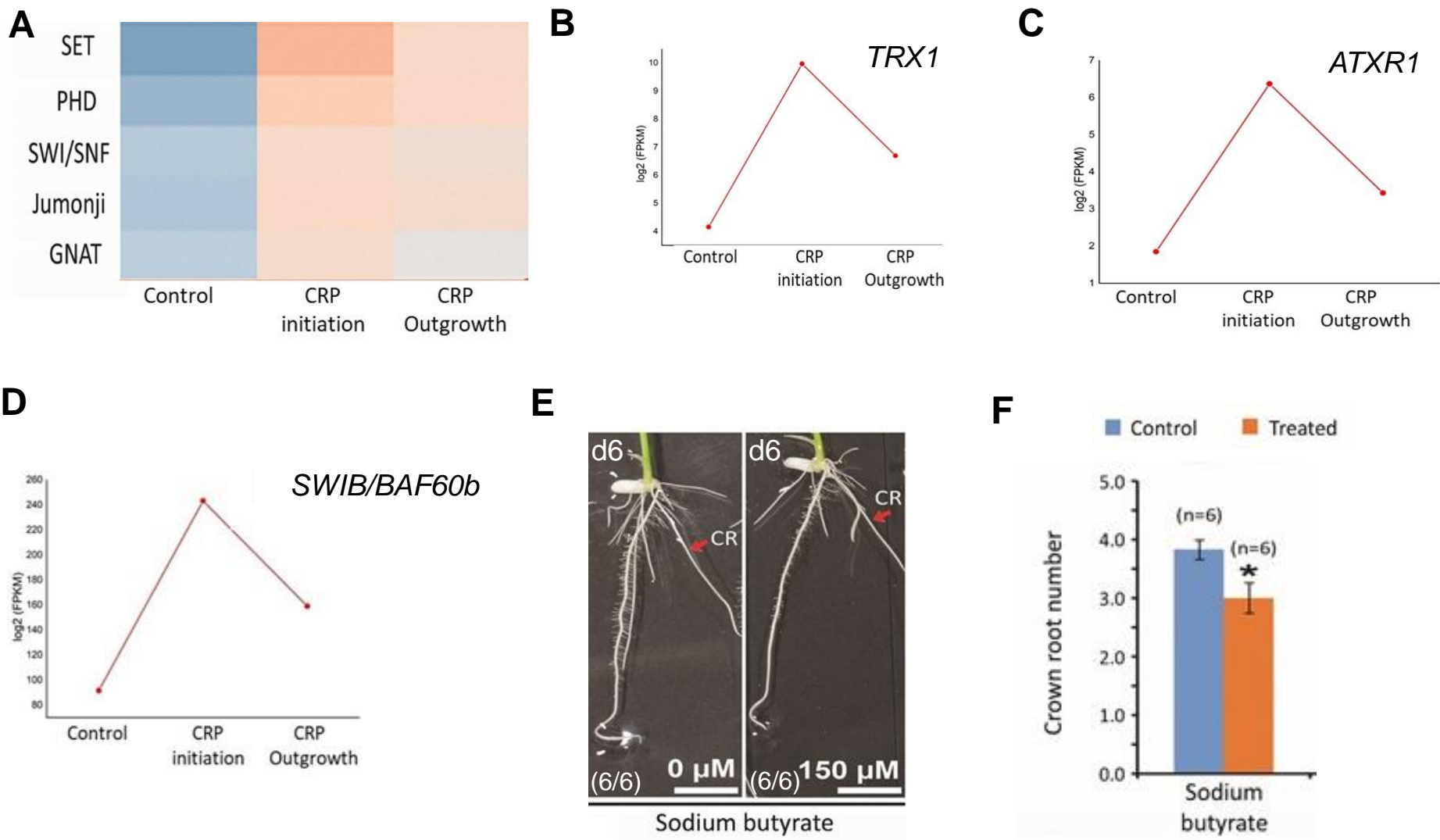


Fig. S4. Epigenetic regulation of CRP development. (A) Geneset enrichment analysis of putative epigenetic regulators.(B-D) LCM-seq expression pattern of selected putative epigenetic modifiers (i.e. *TRX1*, *ATXR6*, and *SWIB/BAF60b*) during CRP initiation and outgrowth. (E,F) CR number was decreased when histone acetylation was interfered for 6 days using sodium butyrate. The mean of CR number is plotted with s.e.m. (**p*≤0.05; two-tailed, unpaired Student's *t*-test). Sample size (n) is mentioned in the panels (E) and (F). Scale bars=1 cm (E).

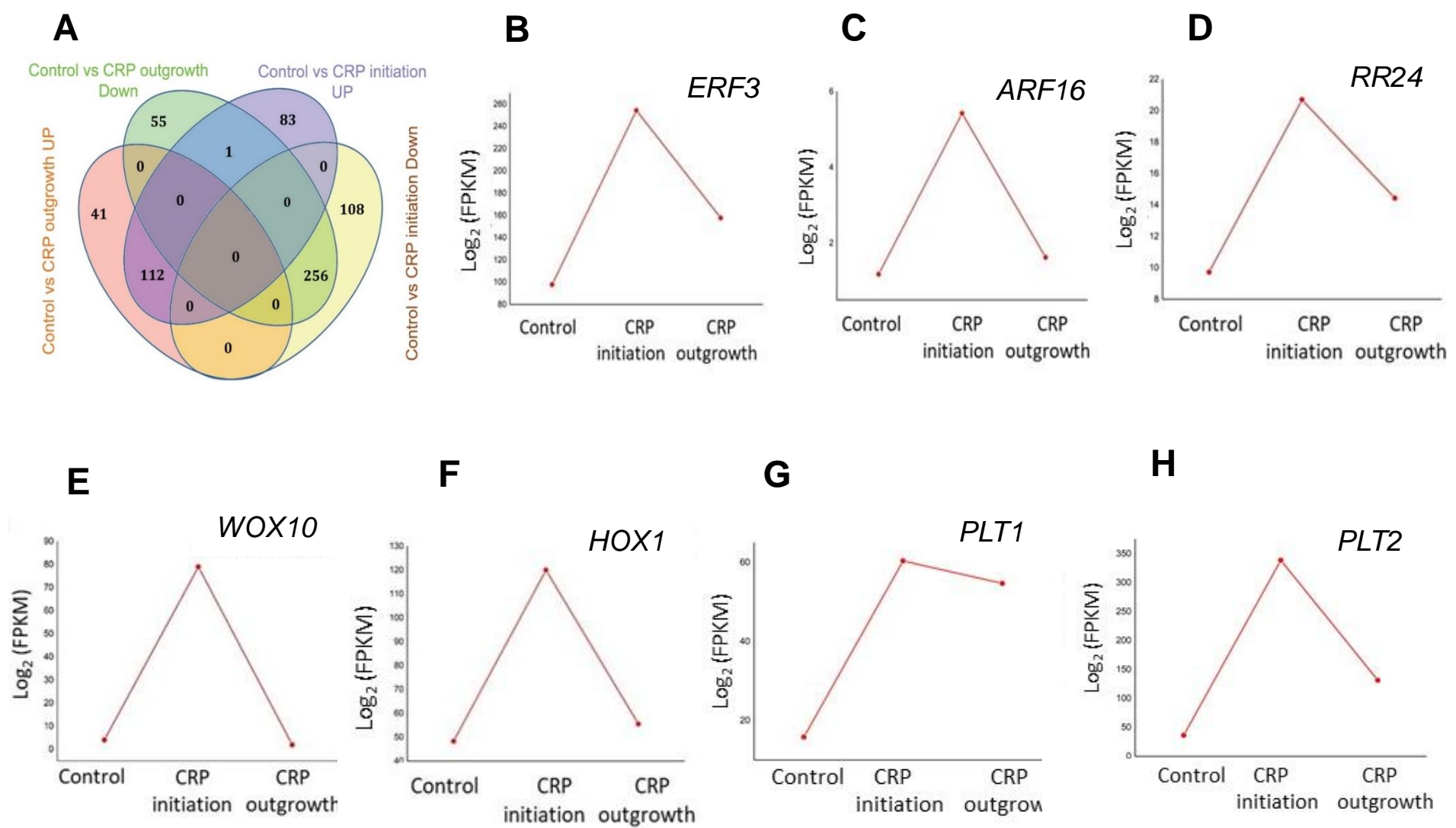


Fig. S5. Differentially regulated transcription factors (TFs). (A) Venn diagram showing common and unique differentially expressed TFs during CRP initiation and outgrowth. (B-H) LCM-seq data for selected TFs (*ERF3*, *ARF16*, *RR24*, *WOX10*, *HOX1*, *PLT1*, and *PLT2*) during CRP initiation and outgrowth.

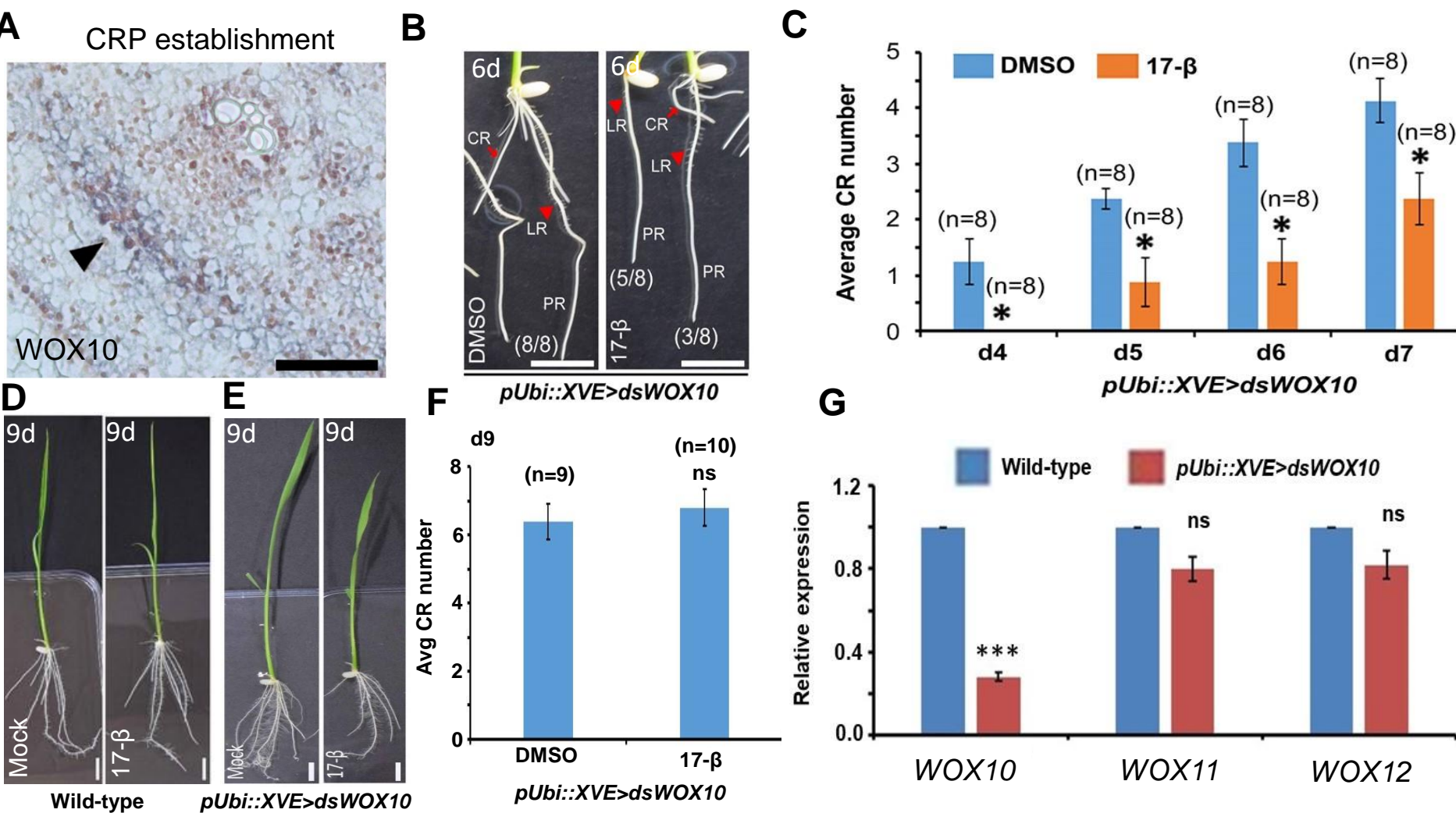


Fig. S6. Functional and molecular characterization of *WOX10* down-regulation lines. (A) *WOX10* expression is initiated in the CR founder cell. (B) CR number is reduced when *WOX10* is down-regulated upon 10 μ M 17 β -estradiol treatment in 6-day old *pUbi::XVE>dsWOX10* lines (right panel) as compared to mock-treated plant (left panel). (C) Quantitative representation of CR number. The mean of CR number is plotted with s.e.m. (* $p \leq 0.05$; two-tailed, unpaired Student's *t*-test). Sample size (*n*) is mentioned in the panels (B,C). (D,E) Plant morphology of 9-day old wild-type (D) and *pUbi::XVE>dsWOX10* lines (E) upon mock (left) and 17- β estradiol (right) treatment. No significant effect was observed in wild-type plants. (F) CR number is not significantly altered in 9-day old *WOX10* down-regulated lines. (G) Down-regulation of *WOX10* upon 17 β -estradiol treatment. Expression level of related *WOX*-genes, *WOX11* and *WOX12* was not affected upon *WOX10* down-regulation. Relative expression (fold change) is plotted with \pm s.e.m. The *p*-value is calculated from three experiments (ns, not significant; $p > 0.05$; *** $p \leq 0.001$; two-tailed, unpaired Student's *t*-test). Scale bars = 25 μ m (A); 1 cm (B,D,E).

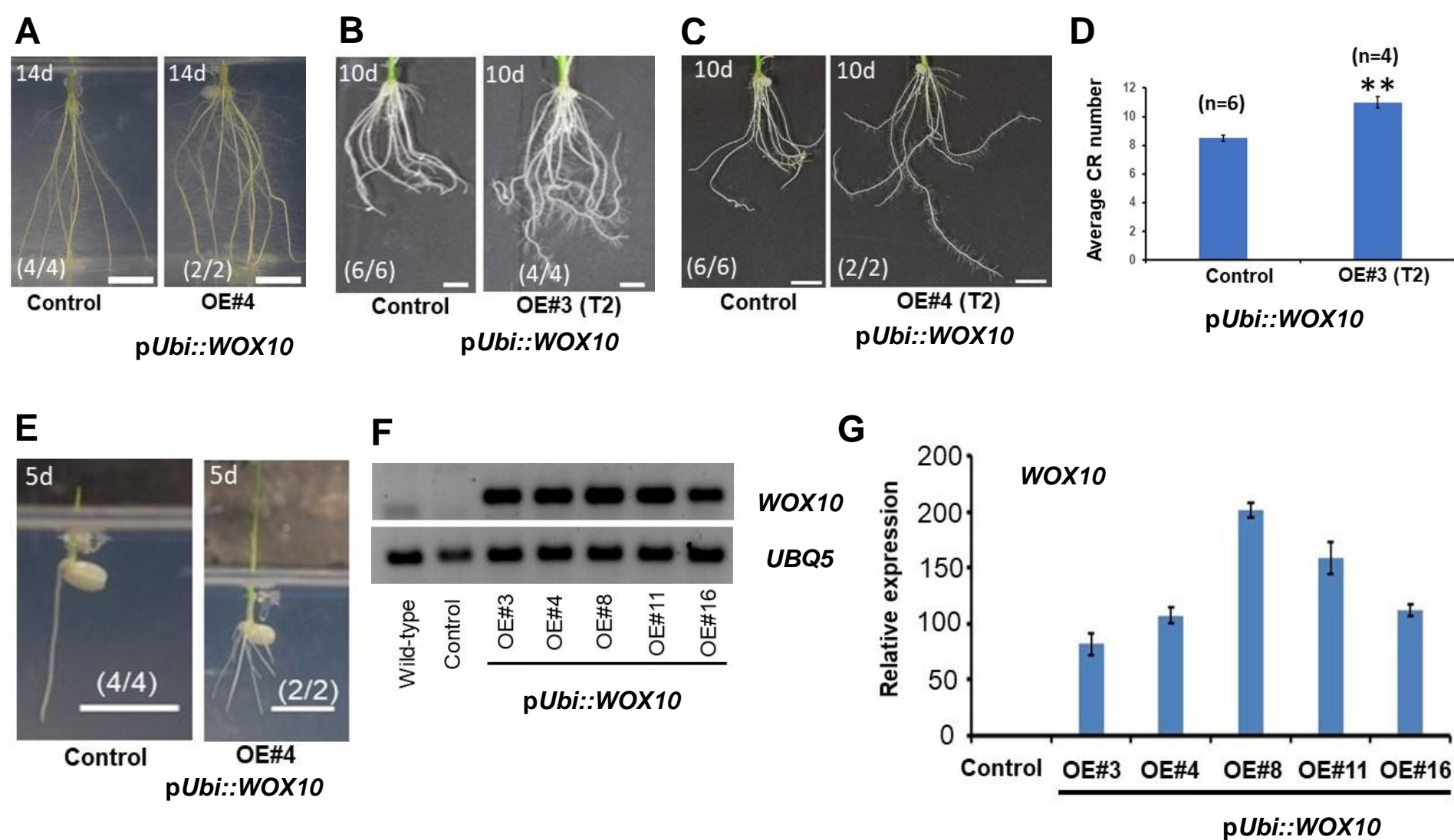


Fig. S7. Functional and molecular characterization of *WOX10* over-expression lines. (A-C) Root architecture of *WOX10* over-expression line OE#4 (T1), OE#3 (T2), and OE#4 (T2). (D) Quantitative representation of CR number. The mean of CR number of 10-day old plantlets is plotted with s.e.m. (** $p \leq 0.005$; two-tailed, unpaired Student's *t*-test). (E) Precocious rooting in 5-day old *WOX10* over-expression line (right), than wild-type (left). Sample size (*n*) is mentioned in the panels (A-E). (F,G) Over-expression of *WOX10* in multiple *pUbi::WOX10* lines, measured by semi-quantitative (F), and qRT-PCR (G). Age of the plants are mentioned at top left side of the panels in (A-C; E). Scale bars = 1 cm (A-C; E).

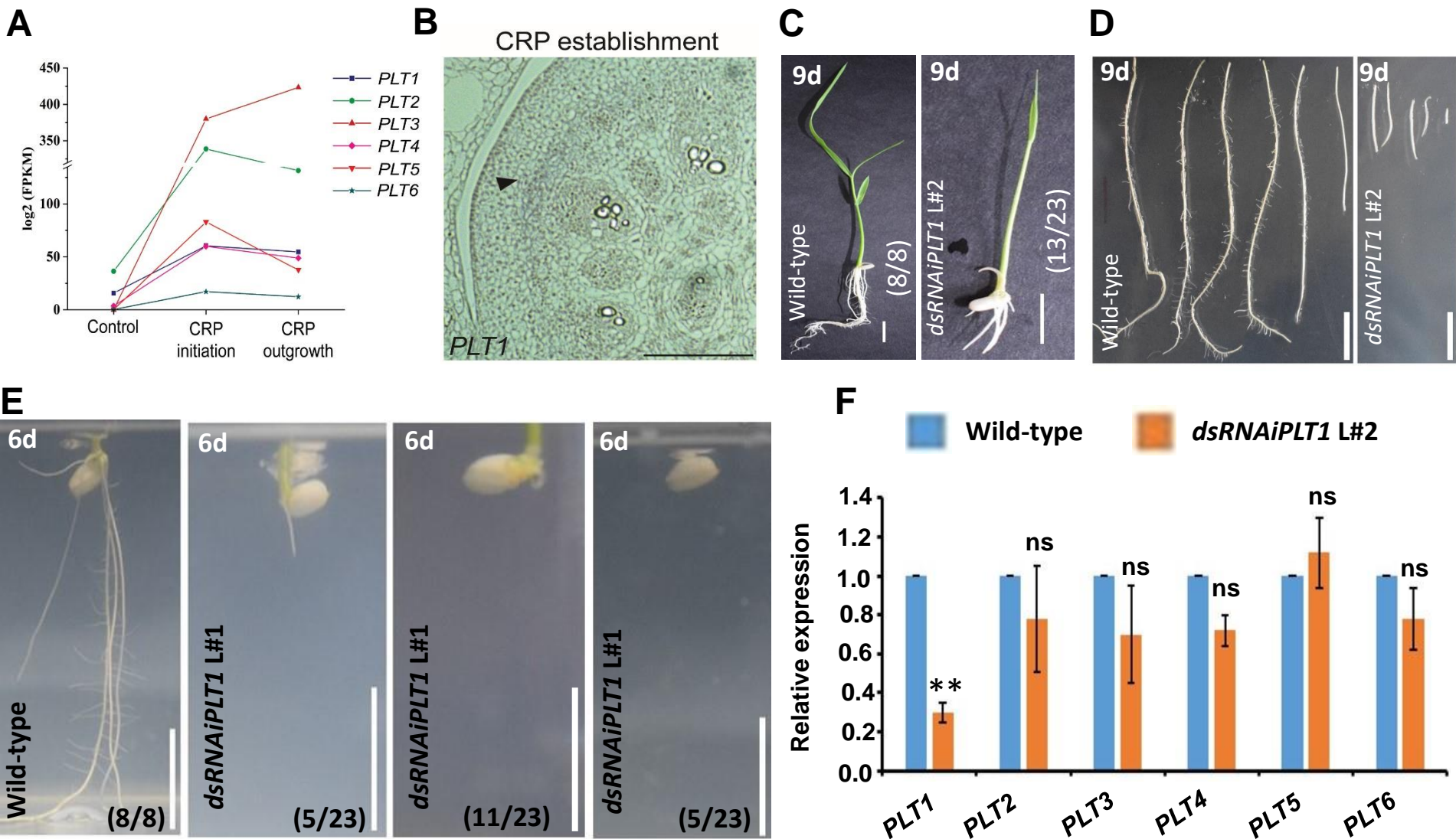
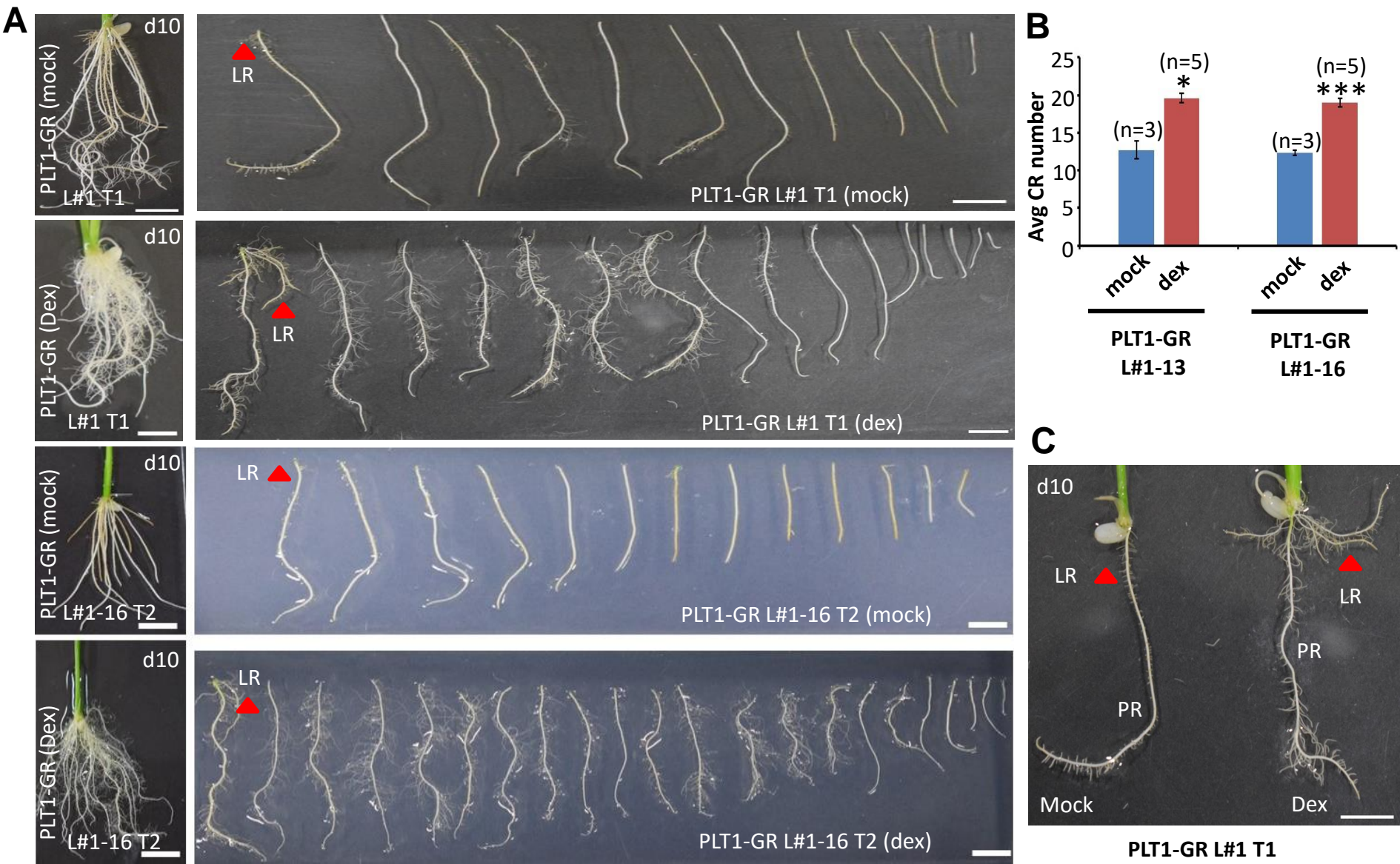


Fig. S8. Phenotypic and molecular characterization of *OsPLT1* down-regulated lines. (A) LCM-seq data for the expression pattern of rice *PLETHORA* genes during CRP initiation and outgrowth. (B) Onset of *PLT1* expression during CRP establishment. (C) Morphology of 9-day old wild-type (left) and *dsRNAiPLT1* L#2 plant (right). (D) LR phenotype of *dsRNAiPLT1* L#2. (E) Phenotypes of 6-day old *dsRNAiPLT1* L#1 plants. Sample size (n) is mentioned in the panels (C,E). (F) Expression level of *PLT* genes, in *dsRNAiPLT1* line. Relative expression (fold change) is plotted with \pm s.e.m. The p-value is calculated from three experiments (** $p < 0.005$; ns, not significant; $p > 0.05$; two-tailed, unpaired Student's *t*-test). Scale bars= 100 μ m (B); 1 cm (C-E).



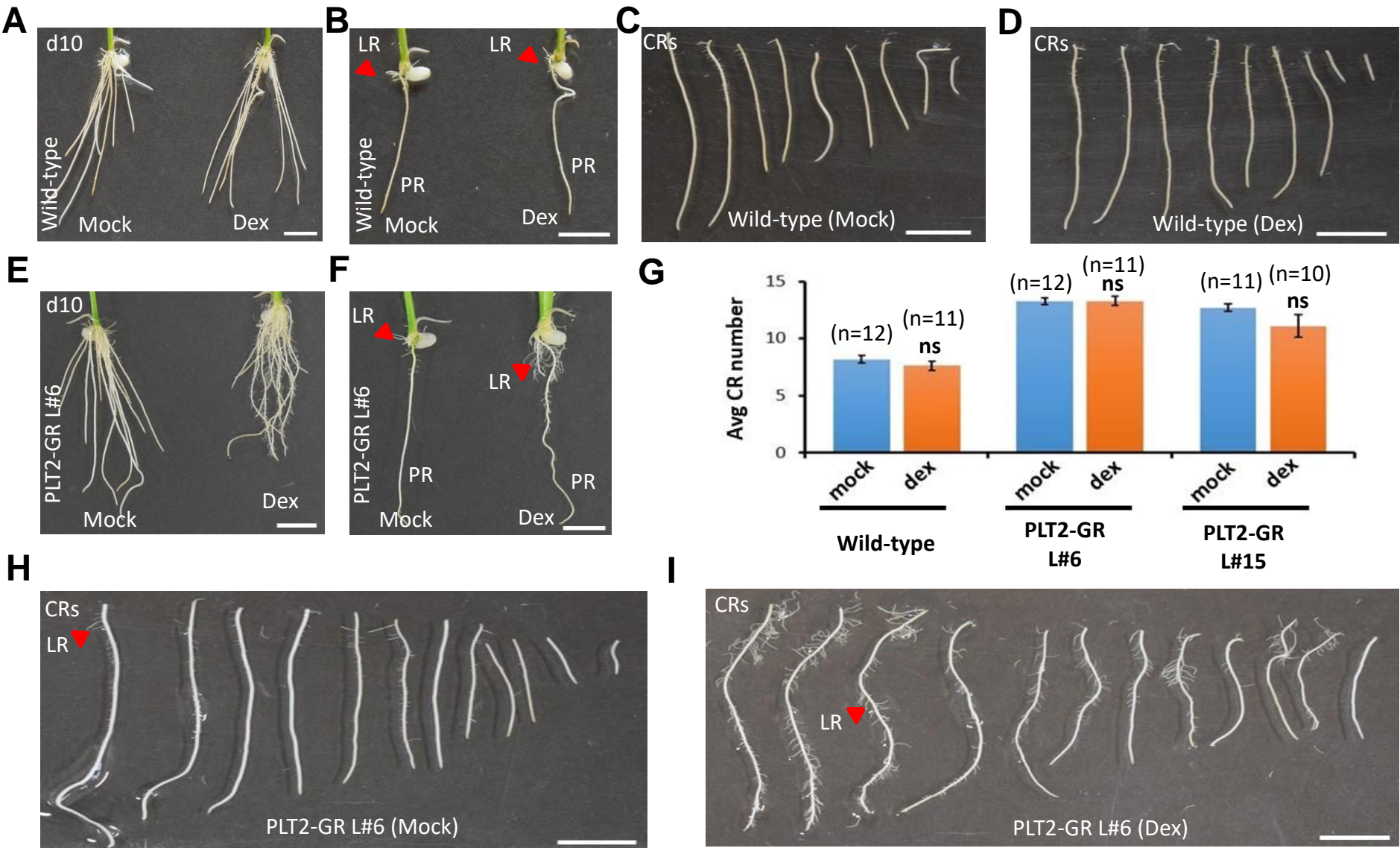


Fig. S10. Phenotypic characterization of *PLT2* over-expression lines. (A) Root architecture upon mock (left) and 5 μ M dex (right) treated 10-day old wild-type plants. (B-D) Dex treatment does not affect LR development on PR (B) and CRs (C,D) of wild-type plants. (E) Root architecture phenotypes of 10-day old *PLT2-GR L#6*. (F) Number and growth of LRs are increased in PR upon dex treatment (right) as compared to mock (left) treated *PLT2-GR L#6* plants. CRs are removed in (B,F). (G) CR number is not affected *PLT2-GR* lines. The mean of CR number is plotted with s.e.m. (ns, $p > 0.05$; two-sample t-test). Sample size (n) is mentioned in (G). (H-I) LR number and growth are increased on the CRs of *PLT2-GR L#6* upon 5 μ M dex treatment. Scale bars= 1 cm (A-F; H,I).

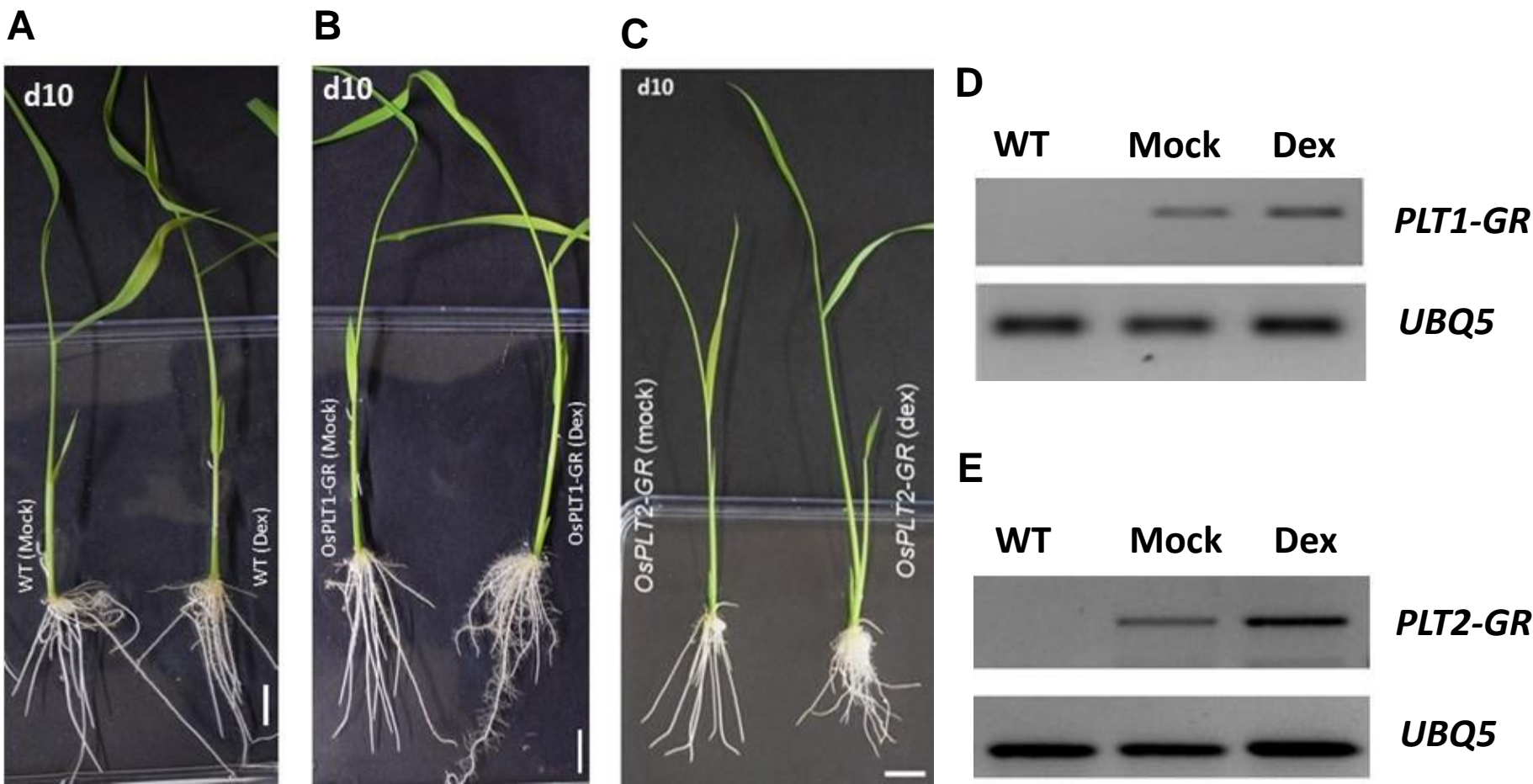


Fig. S11. Molecular and phenotypic characterization of *PLT1* and *PLT2* over-expression lines. (A-C) Plant morphology of 10-day old wild-type (A), *PLT1-GR1* (B) and *PLT2-GR* lines (C) upon 5 μ M dex treatment (right), as compared to mock treated plants (left). No significant effect was seen on the gross morphology of wild-type plants upon dex treatment. (D,E) RT-PCR analysis of *PLT1-GR* and *PLT2-GR* lines, respectively, showing expression of fusion transcripts. Scale bars= 1 cm (A,C).

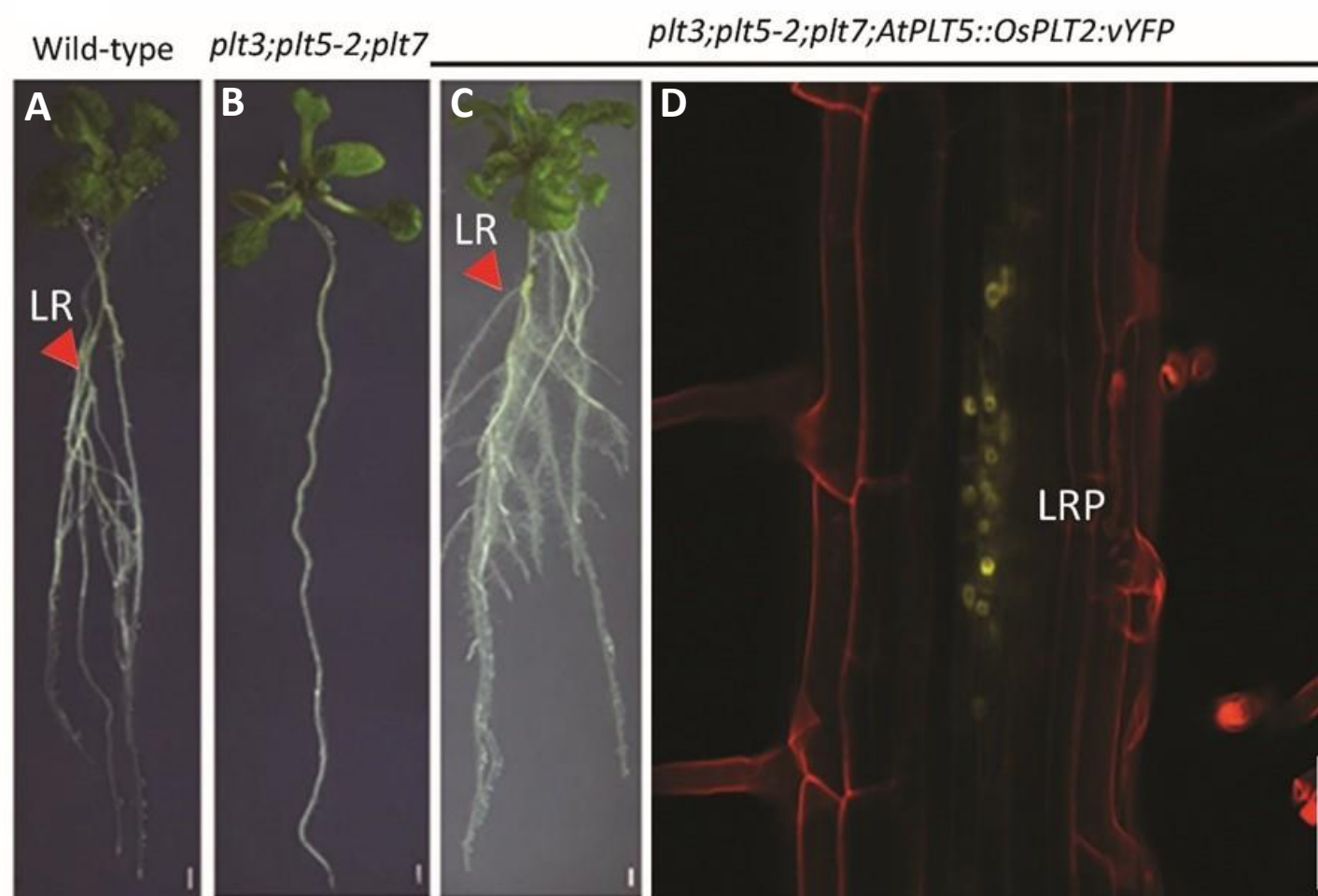


Fig. S12. Expression of *OsPLT2* in lateral root primordia (LRP) of *plt3;plt5-2;plt7* defective in LRP outgrowth rescued LRP outgrowth. Stereo images of 8-dpg wild-type plant (A), *plt3;plt5-2;plt7* (B), and *plt3;plt5-2;plt7;AtPLT5::OsPLT2:vYFP* (C). Confocal images showing expression of *OsPLT2:vYFP* in the LRP of *plt3;plt5-2;plt7;AtPLT5::OsPLT2:vYFP* (D). Red colour in (D) represents propidium iodide staining. (LRP, lateral root primordia; red arrowhead marks LR, lateral root). Scale Bars = 1 mm (A,C); 50 μ m (D).

Table S1. Stage-specific differential expression of known regulators during CRP development

[Click here to download Table S1](#)

Table S2. List of eight annotated clusters of genes with distinct expression pattern during CRP development.

[Click here to download Table S2](#)

Table S3. List of differentially expressed genes during CRP initiation and outgrowth.

[Click here to download Table S3](#)

Table S4. List of specifically and commonly expressed genes during CRP initiation and outgrowth.

[Click here to download Table S4](#)

Table S5. List of putative epigenetic modifiers differentially expressed during CRP development.

[Click here to download Table S5](#)

Table S6. List of genes selected for validation in this study.

[Click here to download Table S6](#)

Table S7. List of differentially expressed transcription factors during CRP initiation and CRP outgrowth.

[Click here to download Table S7](#)

Table S8. List of primers used in this study

[Click here to download Table S8](#)